



UNIVERSIDADE ESTADUAL DE CAMPINAS
Faculdade de Engenharia Química

KAREN JOHANA SILGADO CORREA

INFLUENCE OF THE TURBULENT AND
CONVECTIVE MOMENTUM ON THE
FLAMMABLE CLOUD CALCULATION AND THE
WAVY NATURE DUE TO THE EFFECT OF THE
WIND DIRECTION

INFLUÊNCIA DO MOMENTO TURBULENTO
CONVECTIVO NO CÁLCULO DA NUVEM
INFLAMÁVEL E A NATUREZA ONDULADA
DEVIDO AO EFEITO DA DIREÇÃO DO VENTO

CAMPINAS - SP
2020

KAREN JOHANA SILGADO CORREA

INFLUENCE OF THE TURBULENT AND CONVECTIVE MOMENTUM ON
THE FLAMMABLE CLOUD CALCULATION AND THE WAVY NATURE DUE
TO THE EFFECT OF THE WIND DIRECTION

INFLUÊNCIA DO MOMENTO TURBULENTO CONVECTIVO NO CÁLCULO
DA NUVEM INFLAMÁVEL E A NATUREZA ONDULADA DEVIDO AO
EFEITO DA DIREÇÃO DO VENTO

*Dissertação apresentada à Faculdade de Engenharia
Química da Universidade Estadual de Campinas
como parte dos requisitos exigidos para a obtenção
do título de Mestra em Engenharia Química*

*Dissertation presented to the School of Chemical
Engineering of the University of Campinas in
fulfillment of the requirements for the degree in
Master in Chemical Engineering*

Supervisor: Prof. Dr. Sávio Souza Venâncio Vianna

ESTE TRABALHO CORRESPONDE À VERSÃO FINAL DA
DISSERTAÇÃO DEFENDIDA PELA ALUNA KAREN JOHANA
SILGADO CORREA, ORIENTADA PELO PROF. DR. SÁVIO
SOUZA VENÂNCIO VIANNA

Campinas - SP
2020

Ficha catalográfica
Universidade Estadual de Campinas
Biblioteca da Área de Engenharia e Arquitetura
Rose Meire da Silva - CRB 8/5974

Si34i Silgado Correa, Karen Johana, 1992-
Influence of the turbulent and convective momentum on the flammable cloud calculation and the wavy nature due to the effect of the wind direction / Karen Johana Silgado Correa. – Campinas, SP : [s.n.], 2020.

Orientador: Sávio Souza Venâncio Vianna.
Dissertação (mestrado) – Universidade Estadual de Campinas, Faculdade de Engenharia Química.

1. Dispersão. 2. Fluido dinâmica computacional. 3. Líquidos inflamáveis. 4. Método de Monte Carlo. I. Vianna, Sávio Souza Venâncio, 1975-. II. Universidade Estadual de Campinas. Faculdade de Engenharia Química. III. Título.

Informações para Biblioteca Digital

Título em outro idioma: Influência do momento turbulento convectivo no cálculo da nuvem inflamável e a natureza ondulada devido ao efeito da direção do vento

Palavras-chave em inglês:

Dispersion
Computational fluid dynamics
Flammable liquids
Monte Carlo Method

Área de concentração: Engenharia Química

Titulação: Mestra em Engenharia Química

Banca examinadora:

Sávio Souza Venâncio Vianna [Orientador]
Juliana Puello Méndez
Qingsheng Wang

Data de defesa: 31-08-2020

Programa de Pós-Graduação: Engenharia Química

Identificação e informações acadêmicas do(a) aluno(a)
- ORCID do autor: <https://orcid.org/0000-0002-2442-9608>
- Currículo Lattes do autor: <http://lattes.cnpq.br/5908296375185482>

Folha de Aprovação da Dissertação de Mestrado defendida por KAREN JOHANA SILGADO CORREA, em 31 de agosto de 2020 pela banca examinadora constituída pelos doutores.

Prof. Dr. Sávio Souza Venâncio Vianna

Presidente e Orientador

FEQ / UNICAMP

Videoconferência

Prof. Dr. Juliana Puello Méndez

La Universidad de San Buenaventura

Videoconferência

Prof. Dr. Qingsheng Wang

Texas A&M University

Videoconferência

A Ata da defesa com as respectivas assinaturas dos membros encontra-se no SIGA/Sistema de Fluxo de Dissertação/Tese e na Secretaria do Programa da Unidade

*To God, Mom and Dad.
Yeyo, here we go with another one!*

Acknowledgments

First and foremost to my beautiful God for keeping me in his hands during the hard and wonderful moments, for giving me wisdom during my growth and for keeping my hope alive to achieve my dreams

A very special gratitude to Petr leo Brasileiro S.A. (PETROBRAS) for the total financial support of this research. I thank to the National Petroleum Agency (ANP), Petrobras grant 2017/00577-7, and to FUNCAMP with the protocol 93760-18

I am also grateful to Prof. Dr. Savio Vianna for trusting my abilities, for his knowledge, advise and for being part of my process

I am grateful to my parents Luz and Orlando for being integrally part of my process, for listening to me and encouraging me to give the best of myself everyday, for their love and comprehension. To my siblings Jouseth, Natalia and Steven for being my strength and also I am thankful to my Balu for being a hand and inner support

Thanks are also to my best friend, Tatiele, for being my second hand, and my sister. Without her would have been harder

And finally, last but by no means least, I am grateful to all the encouragement offered from my coworkers at the L4R1S4 lab.

*"Concern for man and his fate must
always form the chief interest of all
technical endeavors. Never forget this in
the midst of your diagrams and
equations."*

Albert Einstein

*"I am among those who think that
science has great beauty."*

Marie Curie

Resumo

Na Análise de Risco de Explosão (*Explosion Risk Analysis* - ERA), os cálculos de ventilação e dispersão usando a Dinâmica dos Fluidos Computacional (*Computational Fluid Dynamics* - CFD) são geralmente considerados quando o nível de confinamento não pode ser negligenciado. Na medida em que a análise de dispersão é considerada, abordagens alternativas são procuradas quando um grande número de simulações é necessário. Definir muitos cenários e simular todos eles nem sempre é adequado dentro do período de tempo do projeto de engenharia real. Como resultado, modelos de dispersão semi-empíricos e vários procedimentos baseados em abordagens estatísticas usando CFD foram propostos para melhorar a robustez e a precisão da previsão do volume da nuvem de gás inflamável. Além do Método de Superfície de Resposta (*Response Surface Methodology* - RSM) e do Método de Nuvem Congelada (*Frozen Cloud Approach* - FCA), é conveniente abordar o problema da dispersão com base na física subjacente à dispersão de um escalar na área dos processos químicos. Seguindo essa linha de raciocínio, foram introduzidos dois modelos matemáticos que predizem a dinâmica de nuvens acidentais depois de vazamentos acidentais de metano. Verificou-se que a nuvem inflamável adimensional estava relacionada à taxa de vazamento acidental, velocidade do vento e do fluido, por meio do equilíbrio entre o momento de liberação e o fluxo do vento convectivo. Resultados numéricos sugeriram uma forma de onda senoidal praticamente alinhada com a função seno cosseno, assim como no círculo trigonométrico. Esta observação está de acordo com a rosa dos ventos a partir de dados meteorológicos. Os modelos matemáticos propostos concordaram muito bem com os dados numéricos calculados usando a dinâmica computacional dos fluidos para certas condições de vento. Finalmente, um caso de estudo considerando o método de Monte Carlo observou-se uma boa aplicação dos modelos desenvolvidos.

Palavras Chaves: Análise de dispersão, previsão de nuvem inflamável, CFD, teorema Pi Buckingham

Abstract

In Explosion Risk Analysis (ERA), ventilation and dispersion calculations using Computational Fluid Dynamics (CFD) are usually considered when the level of confinement and congestion cannot be neglected. As far as the dispersion analysis is considered, alternative approaches are sought when a large number of simulations is required. Setting many scenarios and simulate them all is not always suitable within the time-frame of real engineering design. As a result, semi-empirical dispersion models and several procedures based on statistical approaches using CFD have been proposed to improve the robustness and the accuracy of prediction of the flammable gas cloud volume. Notwithstanding, the use of Response Surface Method (RSM) and Frozen Cloud Approach (FCA), it is convenient to address the problem on the basis of the physics underlying the dispersion of a scalar in the chemical process area. Following this line of reasoning, two mathematical models were introduced for the prediction of accidental flammable clouds after methane releases. It has been found that the dimensionless flammable cloud was related to the accidental leak rate, wind speed, and fluid by means of the balance between the release momentum and the convective wind flow. Numerical findings suggested a sinusoidal waveform pretty much in line with sine-cosine function as in the trigonometric circle. This observation goes in line with the wind rose from meteorological data. The proposed mathematical models agreed very well with numerical data calculated using computational fluid dynamics at certain wind conditions. Finally, one case of study considering Monte Carlo method was used for the application of the proposed model.

Keywords: Dispersion analysis, flammable cloud prediction, CFD, Buckingham Pi theorem.

List of Figures

1.1	The structure of this work	19
2.1	Regions involved in a dispersion event for a continuous release.	22
3.1	Puff formation after an instantaneous rupture	28
4.1	Geometry model and wind direction scheme for a semi-confined module	38
4.2	Leak position and directions represented into the geometry	40
4.3	Geometry meshing for two different leak rates: (a) 0.5 kg/s of leak rate, (b) 500 kg/s of leak rate.	42
5.1	First set of dispersion scenarios: (a) variations of wind direction at up leak jet direction, (b) variations of wind speed at up leak jet direction, (c) and (d) variations of leak rate at up leak jet direction, (e) and (f) variations at different leak directions	49
5.2	Second set of dispersion scenarios only considering variations of wind direction and three fixed values of wind speed of 2, 6 and 8 m/s: (a),(b) and (c) at fixed leak rate of 5 kg/s	50
5.3	Second set of dispersion scenarios only considering variations of wind direction and three fixed values of wind speed of 2, 6 and 8 m/s: (a),(b) and (c) at fixed leak rate of 25 kg/s	50
5.4	Second set of dispersion scenarios only considering variations of wind direction and three fixed values of wind speed of 2, 6 and 8 m/s: (a), (b) and (c) at fixed leak rate of 200 kg/s	51
5.5	Third set of dispersion scenarios only considering variations of wind direction and three fixed values of wind speed of 2, 6 and 8 m/s: (a),(b) and (c) at fixed leak rate of 50 kg/s; (d),(e) and (f) at fixed leak rate of 100 kg/s	52
5.6	Representation of the waveform of the cloud volume based on the dimensional analysis for groups 8B and 8C (refer to Table 4.1)	54

5.7	Comparison of CFD-data based on dimensional analysis with the mathematical model in the determination of \hat{V} at different leak jet direction: (a) Up leak jet direction, (b) Back leak jet direction, (c) Down leak jet direction, (d) Front leak jet direction, (e) Left leak jet direction, (f) Right leak jet direction.	56
5.8	Analysis of the dimensionless volume obtained by CFD data and the values provided by the proposed mathematical model	57
5.9	Accuracy evaluation and model validation of the 120 simulations	59
5.10	Accuracy evaluation and model validation against CFD data, and the model at different values of leak rate (LR) at 6 m/s and 8m/s of wind speed (WS): a) SG4_5, (b) SG5_25, (c) SG7_50, (d) SG8_100.	60
5.11	Geometric mean bias against geometric mean variance	62
5.12	General representation of the flammable cloud behavior within the module after comparing the two dimensionless numbers	64
5.13	Comparison of the relationship of \hat{V} against R for two different wind speeds (2 m/s, and 8 m/s), five leak rates (5, 25, 50, 100, 200 kg/s), eight wind directions (N, S, E, W, SE, SW, NE, NW) and up leak direction	65
5.14	Comparison between $\hat{V}(R)$ model and R at different values of leak rate of 5, 25, 50, 100 and 200 kg/s at 2, 6 and 8m/s of wind speed considering the eight wind directions and at up leak direction.	66
5.15	Compilation of data from Figure 5.14 of model $\hat{V}(R)$ against R for all the wind directions at up leak direction and 8 wind directions.	67
5.16	Comparison between $\hat{V}(R)$ model and R at fixed leak rate of 50 kg/s at 2, 6, 8 and 10 m/s of wind speed considering west wind directions at five leak directions (front, left, right, down, back).	67
5.17	Comparison between $\hat{V}(R)$ model and \hat{V} at different values of leak rate of 25, 48, 72, and 95 kg/s at 1.5 m/s of wind speed considering the eight wind directions and at up leak direction.	70
5.18	Geometric mean bias against geometric mean variance	71
A.1	First set of dispersion scenarios at 70 seconds after the release: variations of wind direction at up leak jet direction with a 2080 m^3 of flammable cloud volume	78
A.2	First set of dispersion scenarios at 70 seconds after the release: variations of wind speed at up leak jet direction with a 2460 m^3 of flammable cloud volume	79

A.3	First set of dispersion scenarios at 70 seconds after the release: variations of leak rate at up leak jet direction with a 1800 m^3 of flammable cloud volume	79
A.4	First set of dispersion scenarios at 70 seconds after the release: variations of leak rate at down leak jet direction with a 520 m^3 of flammable cloud volume	80
A.5	First set of dispersion scenarios at 70 seconds after the release: front leak directions with a 443 m^3 of flammable cloud volume	80
A.6	First set of dispersion scenarios at 70 seconds after the release: up leak directions with a 1780 m^3 of flammable cloud volume	81
B.1	Step 1 in McPEAS Software	89
B.2	Step 2 in McPEAS Software	89
B.3	Step 3 in McPEAS Software	89
B.4	Step 4 in McPEAS Software	89
C.1	Example of compilation of data of model $\hat{V}(R)$ against R for all the wind directions	91

List of Tables

2.1	Pasquill-Gifford stability classes based on atmosphere conditions (BURTON, 1998)	25
4.1	Group distribution for the dispersion simulations	40
5.1	Worst-case scenarios of group 9 at different wind directions for each leak direction (50 kg/s of leak rate and 6 m/s of wind speed)	55
5.2	Sum of absolute errors in the analysis of wake angle variations at up leak direction, different wind speeds and wind directions for a set of scenarios	58
5.3	Group of scenarios used in the validation of the proposed model	59
5.4	Statistical performance and evaluation for groups with 6 m/s of wind speed at values of leak rate specified.	61
5.5	Statistical performance and evaluation for groups with 8 m/s of wind speed at values of leak rate specified.	61
5.6	Values of R calculated based on a R_{ref} to obtain a specific leak rate for the validation analysis	68
5.7	Values of adjustable variables (A and B) for model validation	69
5.8	Statistical performance and evaluation for groups with 1.5 m/s of wind speed (Figure 5.17) at values of leak rate specified	69
A.1	Value of Q9 and \hat{V} for the first set of dispersion scenarios	82
A.2	Value of Q9 and \hat{V} for the second set of dispersion scenarios (part a)	83
A.3	Value of Q9 and \hat{V} for the second set of dispersion scenarios (part b)	84
A.4	Value of Q9 and \hat{V} for the third set of dispersion scenarios	85
C.1	Developed variables for the proposed model at all leak directions	90

Contents

1	Introduction	17
1.1	Purpose	17
1.2	Gas Dispersion Analysis	17
1.3	This Dissertation Project	18
1.4	Objectives of This Work	19
1.4.1	General Objective	19
1.4.2	Specific Objectives	19
1.5	Organization of this Dissertation	20
2	Fundamental Concepts	21
2.1	Introduction	21
2.2	The Dispersion Phenomena: Gas leaks	21
2.3	Flammable Gas Cloud Volume	23
2.4	Parameters Influencing the Cloud Size	23
2.4.1	Ventilation Rate	24
2.4.2	Gas Release	25
3	Cloud Volume Prediction	27
3.1	Introduction	27
3.2	Phenomenological Models in Dispersion Analysis	27
3.2.1	Gaussian Models: Plume and Puff	27
3.3	Review of Methodologies using CFD for Cloud Predictions	28
3.3.1	Final Comments	30
4	Numerical Modeling in Gas Dispersion	31
4.1	Introduction	31
4.2	Computational Fluid Dynamics (CFD)	31
4.2.1	Governing Equations in CFD	32
4.3	FLACS CFD tool for dispersion simulation	35

4.3.1	Calculating Stoichiometric Flammable Gas Cloud Volume (Q9) in FLACS	36
4.4	Numerical Analysis of Gas Dispersion in FLACS	37
4.4.1	Geometry Modeling	38
4.4.2	Leak Conditions	38
4.4.3	Scenarios Outline for Dispersion simulations	39
4.4.4	Simulations Setting Up in FLACS	41
4.5	Dimensional Analysis	42
4.6	Application of the Buckingham Pi Theorem for Gas Dispersion	43
4.6.1	Dimensional Analysis without the Geometry Effects	43
4.6.2	Dimensional Analysis with the Geometry Effects	45
5	Numerical Results and Modeling	48
5.1	Introduction	48
5.2	Numerical Simulations of Dispersion Scenarios	48
5.3	Numerical Modeling	53
5.3.1	Flammable Cloud Volume Modeling: M-01	53
5.3.2	Numerical Analysis for the M-02 Model	62
5.4	The Monte Carlo Method Applied in Dispersion Analysis	71
6	Conclusion and Future Work	74
6.1	Main Findings	74
6.1.1	Recommendations in Future Work	75
6.1.2	Scientific Production	75
A	Additional Numerical Data	78
A.1	Visualization of CFD results	78
A.2	Dimensional results	82
B	Developed Tools for V_f Calculations	86
B.1	Introduction	86
B.2	How to Perform a Case Study with McPEAS?	86
B.2.1	Modeling in CFD	86
B.2.2	Modeling in McPEAS	86
B.3	McPEAS Procedure Execution	87

C	How to Use the M-01 and M-02 Proposed Models?	90
C.1	The M-01 Proposed model	90
C.1.1	The M-02 Proposed Model	90

Chapter1

Introduction

"Science cannot solve the ultimate mystery of nature. And that is because, in the last analysis, we ourselves are a part of the mystery that we are trying to solve"

Max Planck

1.1 Purpose

This work introduces a novel alternative to predict flammable gas cloud sizes. The prediction is based on the physical mechanism that governs the accidental releases to evaluate the resulting downwind transport that leads to large flammable gas cloud volumes. The primary interest consists of study the flammable gas cloud by coupling Computational Fluid Dynamics (CFD) with dimensional analysis.

This dissertation is concerned with developing a mathematical correlation to model the dispersion phenomena with the same level of accuracy of CFD simulations. The focus is not on the statistical, but on the underlying physics that governs the gas dispersion.

A two-deck semi-confined offshore platform module geometry is modeled, and dispersion scenarios were performed by using CFD-FLACS (Flame Accelerator Simulator). The proposed models are assessed, validated with statistical analysis, and implemented in a Monte Carlo code to calculate the flammable cloud volumes. Findings show that models offer very good agreement with CFD.

1.2 Gas Dispersion Analysis

Gas dispersion analysis is a technique for the prediction, evaluation, and prevention of potential accidental losses of flammable or toxic materials prone to cause explosions or fire events. One of the best approaches to evaluate flammable gas cloud volumes is the simulation

of case scenarios using Computational Fluid Dynamics (CFD). In fluid mechanics, CFD is a computational tool that uses numerical methodologies and algorithms to evaluate fluid flows.

This work uses FLACS (Flame Acceleration Simulator), a CFD software specialized in process safety applications to predict the cloud volume through the Q9 method. This Q9 method gives the equivalent fuel air metric or the equivalent stoichiometric gas cloud volume in FLACS (Q9).

In dispersion analysis, the evaluation of scenarios is carried out by determining the most influential parameters. Some investigations (SHI *et al.*, 2018b; AZZI *et al.*, 2016; QIAO; ZHANG, 2010; SHI *et al.*, 2018a), confirmed that the leak rate, leak direction, leak position, wind speed, wind direction, flow, and the release duration affect the cloud volume dynamics. Moreover, Dasgotra *et al.* (2018) considered that the degree of congestion and the wind boundary conditions are relevant factors influencing the gas cloud volume.

In this dissertation, the influential parameters considered are the flow (ρ), geometry (A), wind speed (u), leak rate (\dot{q}), wind direction (β), and the leak direction (θ). This work evaluated the relationship between the influential parameters with the flammable cloud volume. The result of this evaluation led to two dimensionless numbers: a *dimensionless volume* \hat{V} and a *dimensionless leak rate* R .

The final objective of this work is to reduce the computational time in dispersion analysis and propose dispersion models to calculate the flammable cloud volume without performing large numerical simulations.

The computational tool named McPEAS and an MS-Excel template were developed by employing the Monte Carlo approach. With these tools, the flammable cloud volume was calculated quickly for countless scenarios, giving good agreement with the CFD data.

1.3 This Dissertation Project

Throughout this dissertation, a numerical study of dispersion phenomena is presented. Two models are suggested for flammable cloud volume calculations. These models have been implemented in the McPEAS software. This software is a computational tool developed by the Dr. Vianna's laboratory at UNICAMP for probabilistic explosion analysis.

In summary, the structure of this work is organized as follows:

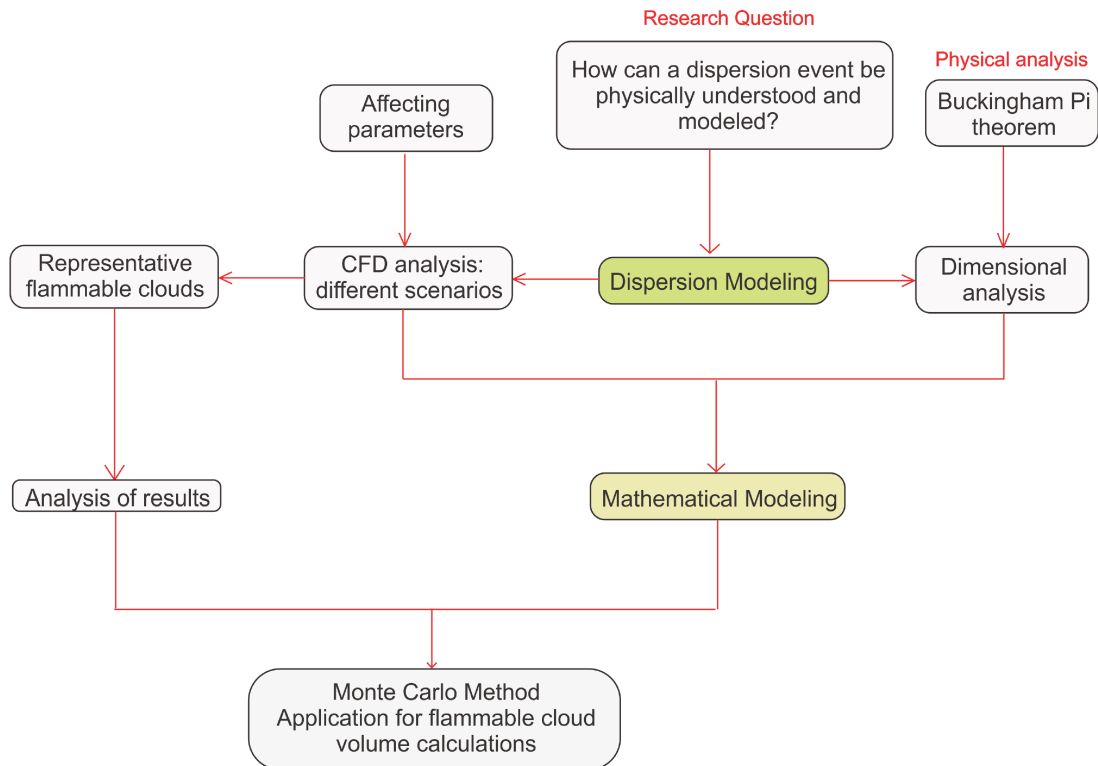


Figure 1.1: The structure of this work

1.4 Objectives of This Work

1.4.1 General Objective

The primary objective is to develop a physics-based model to predict the flammable cloud volume by considering numerical results from dispersion simulations and dimensional analysis.

1.4.2 Specific Objectives

Specific objectives of this study are:

- Perform a dimensional analysis associating the influential parameters of a dispersion with the gas cloud volume using the Buckingham Pi Theorem
- Develop a mathematical procedure to calculate the flammable gas cloud volume
- Implement the proposed procedure applying the Monte Carlo Method for flammable cloud volume calculations

1.5 Organization of this Dissertation

This dissertation discusses flammable gas clouds dispersed into the atmosphere after accidental releases. A brief introduction is addressed in Chapter 1.

In Chapter 2, the basic concepts of gas dispersion phenomena and the parameters influencing the cloud size are addressed.

Chapter 3 covers a review of models and methods used in predicting gas clouds.

Chapter 4 comprises the numerical analysis, the governing equations in CFD, and why FLACS-CFD is widely used in safety applications. The numerical analysis shows how the study and all the calculations were performed. Furthermore, application of the Buckingham Pi Theorem is assessed as well as some considerations regarding the geometry.

Chapter 5 covers the numerical results and the mathematical model development. Numerical findings obtained with the models are compared with the CFD data and then validated with the MEGGE protocol. The models are developed based on the physical understanding of the dispersion phenomena.

Finally, conclusions are presented in Chapter 6. This chapter summarizes all the results obtained and give some recommendations for future work.

Each chapter gives a brief overview of the problem, and provides references for more information.

Chapter2

Fundamental Concepts

*"Imagination is more important than knowledge.
Knowledge is limited. Imagination encircles the
world"*

Albert Einstein

2.1 Introduction

The motion of a flammable cloud after accidental release is described by three different regions: *Source or isolated region*, *the dispersion region* and *passive dispersion* (Figure 2.1). The isolated region covers different source scenarios present in a dispersion (e.g., jet release with high-momentum, two-phase jet, total vessel failure, and leakages in pipes or vessels). The dispersion region describes how environmental conditions affect the flow dynamics, and the passive dispersion is mainly dominated by the surroundings (wind and weather conditions) (DEVAULL *et al.*, 1995).

This chapter provides some fundamental concepts of dispersion. It includes the main stages associated with accidental releases and the importance of determining the influential parameters in the cloud formation. It also gives a brief description of semi-empirical models widely used to assess plume and puff events.

2.2 The Dispersion Phenomena: Gas leaks

In industry, gas leaks are likely to occur in confined spaces (e.g., offshore platform). The initial discharge of a leak is a jet that forms a characteristic plume after mixing with air.

When the fluid disperses into the atmosphere, the clouds formed are under the influence of the wind conditions, atmospheric turbulence, the buoyancy effects, and other major environmental parameters. Likewise, according to CCPS (Center for Chemical Process Safety), the main factors to consider in a dispersion analysis are the source definition, environment conditions, type of release, and the determination of potential release scenarios.

After a release takes place, the pressure difference between the environment and the reservoir will determine the fluid phase (e.g., liquid, vapor, or both). When the pressure difference is small, the flow is subsonic; however, if the pressure difference increases, the fluid behaves like supersonic jet (DEVAULL *et al.*, 1995).

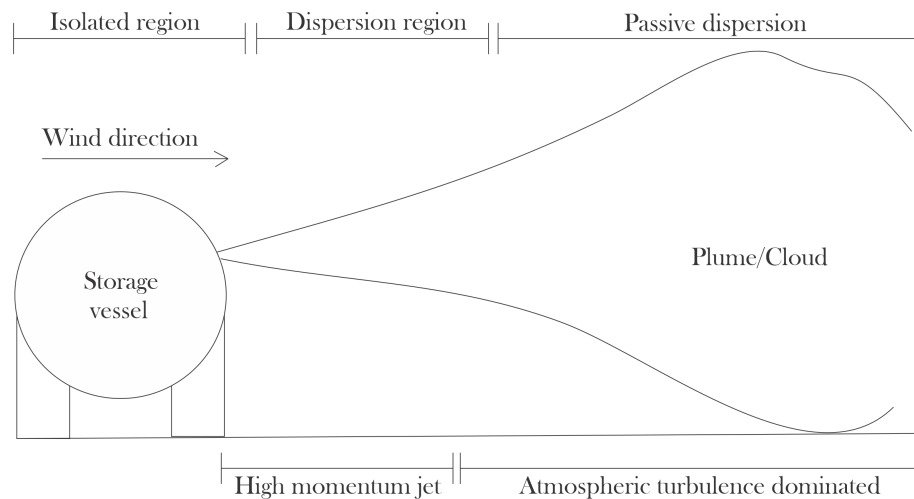


Figure 2.1: Regions involved in a dispersion event for a continuous release.
Adapted from *Chemical Process Safety: Fundamentals with Applications* (CROWL; LOUVAR, 2011)

In Figure 2.1, an example of a jet is shown. The Figure represents the key regions considered in the evaluation of the dispersion phenomena.

- The *source or isolated region*, in this region all the estimates are independent of the environmental conditions. Also, calculations of the mass release rate, release duration, fluid velocity, and fluid density are included
- The *dispersion region* considers the source, the module geometry, and all the environmental conditions to calculate the release trajectory, dilution rate, and the evaporation rate of the release
- In the *dispersion region*, the release condition is subjected to the wind field, which will influence the cloud's path and the dilution rate.
- The *passive dispersion* is mostly dominated by environment mixing where the source size, the wind, and weather conditions define the final trajectory, and the entrainment rate.

It is important to highlight that in the passive dispersion region, the release is governed by the atmospheric turbulence. Hence, the wind will have a limited influence on the dilution of the plume, because the gas concentration will be lower than the gas concentration

at the source of the release (DEVAULL *et al.*, 1995). Thus, the dispersion scenario can be defined by five parameters:

1. Source characteristics — composition, material mass in inventory, thermodynamic properties, and geometry of the leak
2. Environment conditions — air pressure, wind speed, wind direction, atmospheric stability, ambient temperature, relative humidity, obstructions, and ground conditions
3. Type of release — e.g., liquid, gas, vapor, multi-phase or aerosol
4. Potential sources scenarios — e.g., leak in a pipe or vessel, ruptures, and pool fire (liquid evaporation)
5. Dispersion — implies the evaluation of the influence of density, source momentum, and the atmospheric turbulence in the gas dispersion.

2.3 Flammable Gas Cloud Volume

Flammable clouds are formed after flammable gas leaks. When a flammable cloud reaches an ignition point, the flame propagation is only possible if the mixing ratio of fuel air is within the flammability limits.

The flammability limits are determined by the Lower Flammability Limit (LFL) and the Upper Flammability Limit (UFL). To determine whether the cloud represents a potential fire or explosion, the volume percentage (concentration) of the material released needs to be within these limits.

If the fuel concentration is lower than the LFL, the fuel air mixture is too lean to burn. Otherwise, if the fuel concentration is greater than the UFL, it will be too rich to burn (ECKHOFF, 2016). Therefore, not all clouds are likely to ignite. On the other hand, they may be responsible for toxic and health effects.

2.4 Parameters Influencing the Cloud Size

A variety of parameters are involved in a dispersion scenario. These parameters are associated with wind speed, wind direction, leak rate, leak direction, leak location, leak duration, and fluid density. In this section, some parameter's definitions are given.

2.4.1 Ventilation Rate

The ventilation rate is the net airflow passing through a certain region. This parameter includes the influence of the wind direction and the wind speed on the module geometry. It is affected by the presence of surface obstacles that disturb or deviate the flow rate pattern.

Surface obstacles

The presence of obstacles may lead to recirculation zones due to a separation of the boundary layer. This phenomenon plays an important role on the prediction of gas cloud volumes. Thus, the roughness height and the vertical wind profile are more stable as the surface conditions are less congested (i.e., from largely congested to flat surfaces) (DEVAULL *et al.*, 1995).

Wind direction and speed

The influence of the wind direction in the cloud formation varies with the geometry configuration. In congested geometries, the equipment and large obstacles can block the airflow.

For open areas, flammable or toxic atmospheres are reduced due to an increase in the ventilation rate. In regions where the air is not in movement, gases can be accumulated without dilution (SCOTT *et al.*, 2011). This situation explains why the wind direction and wind speed play an important role in the air fuel mixing ratio.

Atmospheric turbulence

Atmospheric turbulence is related to the irregular motion of the fluid flow. The turbulence is the governing mechanism for the dilution (air fuel) into the atmosphere. In dispersion, the atmospheric turbulence is evaluated by the Pasquill-Gifford stability classes categorized under meteorological conditions (refer to Table 2.1).

Mechanical Turbulence and Class Stability

The mechanical turbulence indicates the effect of the roughness height on the wind profile. The roughness is classified based on the type of area (e.g., flat, ice, urban, mountains).

An increment of roughness height along with high values of wind speed will increase the grade of turbulence in the atmosphere.

On the other hand, in stratified flows, vertical air density changes will affect turbulent mixing.

The distribution of density variations depends on the atmospheric conditions of the ground. These conditions are characterized by the averaged vertical density and temperature as neutral, stable, and unstable, as illustrated in Table 2.1 (DEVAULL *et al.*, 1995).

Table 2.1: Pasquill-Gifford stability classes based on atmosphere conditions (BURTON, 1998)

Pasquill-Gifford stability classes						
Surface wind speed (m/s)	Day with insolation			Night		
	Strong	Moderate	Slight	Overcast or $\geq 4/8$ low cloud	$\leq 3/8$ cloud	
2	A	A-B	B	-	-	
2-3	A-B	B	C	E	F	
3-5	B	B-C	C	D	E	
5-6	C	C-D	D	D	D	
6	C	D	D	D	D	

A: Extremely Unstable; B: Moderately Unstable; C: Slightly Unstable; D: Neutral; E: Slightly Stable; F: Moderately stable.

There are different methods to quantify the conditions in the atmosphere. One of the most used for dispersion modeling is the Pasquill-Gifford method. This method classifies the atmospheric stability by requiring an estimate of wind speed and the surroundings (day or night).

The categorization of this method is from A to F (Table 2.1). Nonetheless, this approach is valid only when the turbulence mixing dominates the dispersion, and when the distances from the release cover from 0.1 to 10 km (CROWL; LOUVAR, 2011).

2.4.2 Gas Release

Gas density

Air density alters the turbulent mixing in the lower atmosphere. This parameter represents the interaction of the buoyancy forces with the mixing ratio between air and gas.

Leak rate and direction

The leak rate relates to the amount of gas released over time, and the duration is dependent on the reservoir volume, orifice size and differential pressure. When the leak

direction is opposite to the wind direction, the interaction air-fuel will generate large clouds due to the formation of recirculation zones (DEVAULL *et al.*, 1995).

Chapter3

Cloud Volume Prediction

"Science knows no country, because knowledge belongs to humanity, and is the torch which illuminates the world."

Louis Pasteur

3.1 Introduction

This chapter summarizes the models applied to gas dispersion (i.e., phenomenological, statistical, neural, and CFD models). In this work, special attention is given to CFD models. The literature review shows the studies performed using Computational Fluid Dynamics (CFD) to develop procedures for the prediction of gas cloud volumes.

3.2 Phenomenological Models in Dispersion Analysis

3.2.1 Gaussian Models: Plume and Puff

After accidental leaks, a recirculated region is formed near the initial discharge that allows the jet to mix with the air. Plume and puff models are experimental-based neutrally buoyant models applied to gases at low concentrations and are used to estimate the downwind concentration in accidental releases.

Plume models represent the steady-state concentration of a release from a continuous source. This continuous release is similar to a smokestack, which forms a large plume, as seen in Figure 2.1 (CROWL; LOUVAR, 2011).

On the other hand, puff models describe a temporal concentration from a single release based on a specific volume of material. This is because a total rupture presented in a puff event (Figure 3.1).

In this context, observing the phenomena, a plume can also be defined as a sequence of continuous puffs. Hence, plumes can also be modeled with the puff models. The evaluation

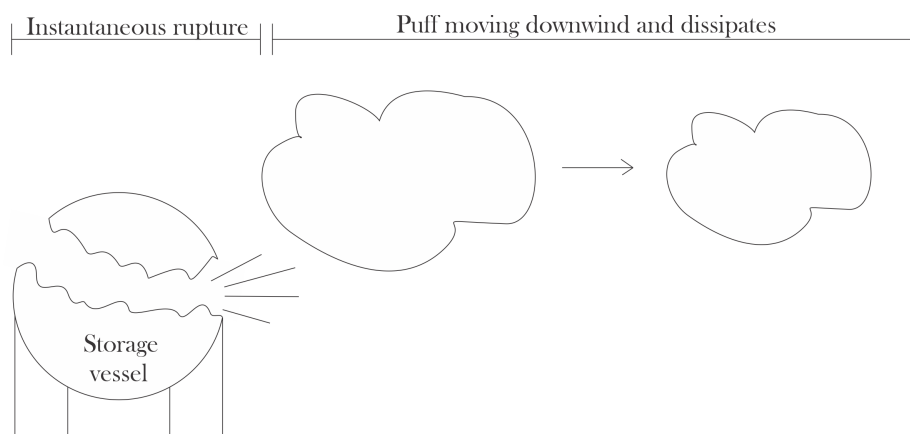


Figure 3.1: Puff formation after an instantaneous rupture

Adapted from *Chemical Process Safety: Fundamentals with Applications* (CROWL; LOUVAR, 2011)

of a plume using puff models is useful when the information requires a steady-state plume. In other cases, when there is an interest in knowing the effect of the wind direction in the cloud, plume models should be used.

Both plume and puff models describe the phenomena by calculating an average concentration of the cloud volume under applicable conditions. These conditions are related to wind characteristics, eddy diffusivity, transient or steady-state releases, and finally, the source (CROWL; LOUVAR, 2011).

3.3 Review of Methodologies using CFD for Cloud Predictions

A variety of methodologies have been used to predict flammable cloud volumes after accidental releases. The methodologies include the development of dispersion models (e.g., statistical, empirical, and integral) using CFD (FIATES; VIANNA, 2016; FERREIRA; VIANNA, 2014; FERREIRA *et al.*, 2019), and the novel Neural Network approach (SHI *et al.*, 2018a).

Likewise, the utilization of DEGADIS and FEM3A models has been considered. For instance, Spicer & Havens (1996) analyzed the DEGADIS model sensitivity for the prediction of gas releases and wind speed. For this investigation, the scope of the models showed some limitations. The prediction with DEGADIS only considered the evaluation of near source behavior, short distances around 100 m, and limited mass estimates.

On the other hand, Shi *et al.* (2018b) evaluated the complex relationship between

the influential parameters and the flammable cloud. In this research, a dispersion event was modeled with a robust polynomial equation by calculating several statistical features. The features were associated with the total number of simulations, and the number of parameters; however, the main disadvantage lied in the model accuracy depending on the number of simulations performed.

Regarding the neural network applications for flammable cloud prediction, Shi *et al.* (2018a) investigated the agreement of two data-driven models. The Bayesian Regularization Artificial Neural Network (BRANN) and the Levenberg-Marquardt Artificial Neural Network (LMANN) were examined. Shi *et al.* (2018a) compared three different numerical models (BRANN, LMANN, and RSM) to study the dispersion in a congested geometry. They used a systematic methodology (structured framework in five steps) to verify and assess the efficiency of those techniques in dispersion modeling.

The developed BRANN model in the research, resulted in the most robust, more accurate than FCA, and a good alternative for flammable cloud volume estimates. However, transient values of Q9 (equivalent fuel-air cloud representation used in FLACS), Q6 (FLACS parameter), and FLAM (Flammable cloud in FLACS) were not studied but recommended.

In the analysis of transient releases, Gupta & Chan (2016) proposed a methodology using time-varying release rates, and reduce the time in performing an ERA (Explosion Risk Analysis). Results showed that the use of a pseudo-transient analysis under predicts the Q9 for smaller cloud volumes and over predicts the bigger ones.

Nonetheless, the accuracy of the model obtained in full transient release rates relied only on representative sections in the facility (GUPTA; CHAN, 2016). This disadvantage indicates that the methodology is not reliable, because the analysis of incidents in the facility should cover all the potential areas. Moreover, the computational cost will increase considerably.

Another scheme in evaluating clouds was proposed by Jin & Jang (2018). The study consisted in evaluating the cloud frequency distribution of the CFD simulations considering time-varying leak rates. In this last research, the procedure was accurate, but the evaluation of processes (constant or transient) for a gas cloud propagation without having a significant increase in the total computational cost or any overestimation is still a burden to control.

3.3.1 Final Comments

Most of the research work about dispersion phenomena are based on a statistical approach and the consideration of the underlying physics is not clearly evaluated. Based on this fact, some gaps in the field of dispersion modeling are listed:

- The models for cloud volume prediction are not robust. Some of them are only applicable to certain conditions (e.g., phenomenological models)
- CFD analysis is expensive as it requires professional expertise and extensive computational effort
- Lack of the physical understanding of the phenomena because the current applications are mostly based on statistics

Chapter4

Numerical Modeling in Gas Dispersion

*“Education is not the learning of facts, it’s rather
the training of the mind to think.”*

Albert Einstein

4.1 Introduction

This chapter provides fundamental concepts related to the fluid flow that can be used for numerical and mathematical modeling of the gas dispersion phenomena. It includes the methodology in the numerical analysis, information about the FLACS CFD package applied for dispersion simulations, and the application of the Buckingham Pi Theorem to perform a dimensional analysis.

In this chapter, the numerical methodology comprises the geometry modeling, leak conditions, scenarios performed for the dispersion analysis, and the setting up in FLACS.

4.2 Computational Fluid Dynamics (CFD)

Computational Fluid Dynamics (CFD) is the widely used numerical tool for academics and industry to estimate and represent a physical phenomena.

CFD provides numerical solutions by calculating the governing equations for fluid flows. These sets of equations given by the Navier-Stokes equations are the continuity equation and some additional conservative equations.

Furthermore, CFD is also used for validation of experimental results and for industrial applications in simulating real scenarios with a numerical modeling approach. Codes in CFD are composed of different elements, including geometry design, pre-processing, and post-processing.

A CFD analysis includes five main steps that are associated with the numerical procedure and the geometry under study:

1. Mathematical modeling — includes the understanding of the phenomena and identifying the governing equations of the process

2. Geometry — geometry design
3. Pre-processing — is subdivided into two main steps: grid construction and model set up. The grid construction refers to the computational domain's discretization; and the model set up to the definition of the simulation conditions. Both based on the geometry design and the mathematical modeling
4. Solver — solution of the governing equations
5. Post-processing — analysis of the results

The application of CFD to solve fluid dynamic problems is growing, especially for experimental tests that cannot be easily performed on a real scale. This situation makes CFD a reliable alternative for numerical calculations of fluid flows.

4.2.1 Governing Equations in CFD

In fluid mechanics, the governing equations for fluid flows obey the generalized conservation principle. These conservative equations (e.g., mass, momentum, energy) are applied upon the fluid under study.

Thus, by taking a variable ϕ to represent a dependent general conservative variable for all fluid flow equations in a differential form (PATANKAR, 1980):

$$\frac{\partial(\rho\phi)}{\partial t} + \text{div}(\rho\phi u) = \text{div}(\Gamma_{\phi} \text{grad } \phi) + S_{\phi} \quad (4.1)$$

Here, Γ_{ϕ} is the diffusion coefficient and S_{ϕ} the source term.

The variable ϕ represents the quantities of mass fraction, enthalpy or temperature, velocity component, or the ones related to turbulence (turbulence kinetic energy or turbulent length scale). The employment of one of these variables will affect the variable S , the coefficient Γ because both depend on the variable ϕ .

Mass Conservative Equation

The conservation of mass considers that the mass variations into the control volume must be entirely due to the inflow or outflow of mass through ΔV (VERSTEEG; MALALASEKERA, 2007).

$$\frac{\partial}{\partial t} \int_{cv} \phi \rho dV = - \int_{cv} \phi \rho \vec{u} \cdot \vec{n} dS \quad (4.2)$$

Where from the sum of all flows in all areas:

$$\frac{\partial}{\partial t} \int_{cv} \phi \rho dV + \phi \rho V dA = 0 = \sum_{phases} \quad (4.3)$$

Now considering the flow mass rate ρVA in the control volume,

$$\frac{\partial}{\partial t} \int_{cv} \phi \rho dV + \int_{cv} (\phi \rho \vec{u}) dA = 0 \quad (4.4)$$

Applying Gauss's divergence theorem,

$$\frac{\partial}{\partial t} \int_{cv} \phi \rho dV + \int_{cv} \text{div}(\phi \rho \vec{v}) dV = 0 \quad (4.5)$$

$$\int_{cv} \frac{\partial}{\partial t} \phi \rho dV + \int_{cv} \text{div}(\phi \rho \vec{v}) dV = 0 \quad (4.6)$$

$$\int_{cv} \left(\frac{\partial \phi \rho}{\partial t} + \text{div}(\phi \rho \vec{v}) \right) dV = 0 \quad (4.7)$$

The continuity equation consists of two terms, a convective term as the net flux through the boundaries of the control volume, while the transient term is the accumulation term in the same control volume.

The mass conservative equation or the *continuity equation* in a differential form for any ϕ is given by:

$$\frac{\partial(\phi \rho)}{\partial t} + \text{div}(\phi \rho \vec{u}) = 0 \quad (4.8)$$

Momentum Conservative Equation

The momentum equation is the application of the second Newton's law to an element of fluid. This equation represents the momentum variation in respects to the fluid acting forces.

The total momentum in a volume V , is the integral volume for the product ρu . At any position in the surface, the force exerted by the fluid out of the volume is given by the product between the pressure P and the area S of the face. Thus, it is:

$$\frac{\partial}{\partial t} \int_{cv} \rho \vec{u} dV + \int_A (\rho \vec{u} \phi) \cdot \vec{n} dA = \int_A (\rho \Gamma_\phi \phi) \cdot \vec{n} dA + \int_{cv} S_\phi dV \quad (4.9)$$

Applying Gauss's divergence theorem,

$$\int_{cv} \frac{\partial(\rho \vec{u})}{\partial t} dV + \int_{cv} \text{div}(\rho \phi \vec{u}) dV = \int_{cv} \text{div}(\Gamma_\phi \text{grad}(\rho \phi)) dV + \int_{cv} S_\phi dV = 0 \quad (4.10)$$

$$\frac{\partial(\rho \vec{u})}{\partial t} + \text{div}(\rho \phi \vec{u}) = \text{div}(\Gamma_\phi \text{grad}(\rho \phi)) + S_\phi \quad (4.11)$$

The momentum equation consists of four terms:

The rate of change of ϕ in the fluid element over time (transient term), the total flow of ϕ outside the fluid element (convective term), the increase rate of ϕ due to viscous forces (diffusive term), and the increase rate of ϕ due to other forces (source term) (MALISKA, 2004).

Energy Conservative Equation

The energy equation has different applications depending on the process under study. By considering a negligible dissipation factor, the energy equation is written as (PATANKAR, 1980):

$$\text{div}(\rho u h) = \text{div}(k \text{grad} T) + S_h \quad (4.12)$$

Where k is the thermal conductivity and h the enthalpy, T the temperature and S_h the volumetric rate of heat generation. Now, knowing that $c \text{grad} T = \text{grad} h$, the equation becomes:

$$\operatorname{div}(\rho u h) = \operatorname{div}\left(\frac{k}{c} \operatorname{grad} h\right) + S_h \quad (4.13)$$

and with $h = cT$ with c the constant-pressure specific heat, we have

$$\operatorname{div}(\rho u T) = \operatorname{div}\left(\frac{k}{c} \operatorname{grad} T\right) + \frac{S_h}{c} \quad (4.14)$$

The $k - \varepsilon$ turbulence model

The standard $k - \varepsilon$ model defines a velocity scale and a length scale by using k and ε . This model is considered numerically robust for some industrial applications, and the transport equations are described as (ANSYS, 2011):

For k ;

$$\frac{\partial(\rho k)}{\partial t} + \rho k(\nabla \cdot u) = \operatorname{div}\left(\frac{u_t}{\sigma_k} \nabla k\right) + 2\mu_t S_{ij} \cdot S_{ij} + \rho \varepsilon \quad (4.15)$$

For ε ;

$$\frac{\partial(\rho \varepsilon)}{\partial t} + \rho \varepsilon(\nabla \cdot u) = \operatorname{div}\left(\frac{u_t}{\sigma_\varepsilon} \nabla \varepsilon\right) + C_{1\varepsilon} \frac{\varepsilon}{k} 2\mu_t S_{ij} \cdot S_{ij} - C_{2\varepsilon} \rho \frac{\varepsilon^2}{k} \quad (4.16)$$

These two equations have a convective, diffusive, a rate of production and a rate of destruction for both ε and k (VERSTEEG; MALALASEKERA, 2007).

4.3 FLACS CFD tool for dispersion simulation

The Flame Accelerator Simulator (FLACS) is a specialized tool for safety applications that performs engineering calculations based on a three-dimensional CFD code.

FLACS solves different transport equations for mass, momentum, enthalpy (h), turbulent kinetic energy (k), rate of dissipation of turbulent kinetic energy (ε), mass-fraction of fuel (Y_F), and mixture-fraction (ξ), considering the Favre-averaged transport equations, and the finite volume method (FVM) (GEXCON, 2018).

This tool also includes the standard $k - \varepsilon$ model to evaluate the turbulence effects and the conservative Reynolds Average Navier-Stokes (RANS) equations. All of them used a structured rectangular Cartesian grid, which is the default configuration on FLACS. Moreover, the determination of velocity, density, pressure, and temperature are upon staggered and cell-centered grids.

The difference between FLACS with other CFD tools is that FLACS uses a distributed porosity processor to represent complex geometries. The large objects are defined on-grid, while the small ones as a sub-grid. This approach allows the porosity processor to establish on FLACS an area and a volume to each cell grid. The area and volume attributed include the sub-grid objects in calculations. This condition is helpful to simulate turbulence generation conditions (GEXCON, 2018).

For dispersion simulations, FLACS represents the flow in the atmospheric boundary layer forcing the wind speed, the wind direction, temperature, and turbulence parameters on the inlet boundaries. This feature implies that the atmospheric profile must be set under the influence of atmospheric stability classes (the Pasquill class or the Monin-Obukhov length) (GEXCON, 2018).

The exposition to flammable materials due to confinement, increases the risk of having loss of toxic or flammable chemicals in offshore platforms. The probability of the formation of flammable or toxic clouds needs to be known (KANG *et al.*, 2016).

In the case of flammable materials, when they are combusted, a gas explosion will occur; as a result, blast pressure and all toxic gases dispersed would cause large losses (KANG *et al.*, 2016).

Considering these possible events, the software CFD-FLACS performs 3D large-scale simulations to estimate the equivalent stoichiometric gas cloud volume (Q9) in a determined facility for a process under study.

4.3.1 Calculating Stoichiometric Flammable Gas Cloud Volume (Q9) in FLACS

In the study of accidental discharges, CFD-FLACS has been widely used to evaluate the formation of flammable clouds. For dispersion analysis, FLACS can calculate the stoichiometric fuel air gas cloud volume (Q9).

The Q9 model represented by the Equation 4.17 is a scaled volume that considers

the laminar burning velocity and the volume expansion ratio.

$$Q^9 = \frac{\sum_{i=1}^n V_i [V_e(ER_i) - 1] ERfac(ER_i)}{\max[V_e(ER) - 1] ERfac(ER) : ER_{LFL} \leq ER \leq ER_{UFL}} \quad (4.17)$$

Where ER is equivalence ratio, and V_i is the representation of the summation over all the control volumes i^{th} of the numerical grid inside the gas monitor region.

Furthermore, the fuel air is within the lower flammability limit (LFL) and the upper flammability limit (UFL). That is $ER_{LFL} \leq ER \leq ER_{UFL}$; $V_e(ER_i)$.

According to Gexcon (2018), the V_i is the volume open for fluid flow in the control volume, where ERfac (ER) (Equation 4.18) is between 0 and 1, S_L is the laminar burning velocity, and $V_e = \frac{V_{burn}}{V_{unburnt}}$.

$$ERfac(ER_i) = \frac{S_L(ER_i)}{\max[S_L(ER) : ER_{LFL} \leq ER \leq ER_{UFL}]} \quad (4.18)$$

When $ER = ER_{LFL}$ or $ER = ER_{UFL}$, ERfac (ER) is 0; for $ER = ER_{top}$, ERfac (ER) is 1. For the flammable range, ERfac (ER) is the laminar burning velocity profile scaled to the maximum of one, while it is zero outside the flammable range (GEXCON, 2018).

In Equation 4.17 and 4.18, the volume expansion ratio and laminar burning velocity are two key factors for representing the inhomogeneous fuel air cloud as a homogeneous fuel air cloud in Q9 model. Simulation results led to the equivalent stoichiometric gas cloud volume (Q9) value, a scaled volume that considers the effect of burning velocity and expansion ratio.

4.4 Numerical Analysis of Gas Dispersion in FLACS

The dispersion analysis comprised the simulation of different scenarios of methane release in an offshore platform. Overall, this study was performed in the following steps:

- Geometry modeling
- Evaluation of leak conditions
- Scenarios outline for FLACS simulations

- Simulation calculations: Meshing, setting up of scenarios in FLACS
- Simulation results: Stoichiometric Equivalent Cloud Volume (Q9) values

4.4.1 Geometry Modeling

A two-deck semi-confined platform geometry was modeled measuring 35.95 *m* length, 12.00 *m* width, and 26.60 *m* height. The 3D geometry that belongs to the Figure 4.1 built-in FLACS had an initial coordinate located at (-0.1, -11.5, -0.6).

In the geometry, the wind rose was located based on Figure 4.1 and eight directions were evaluated.

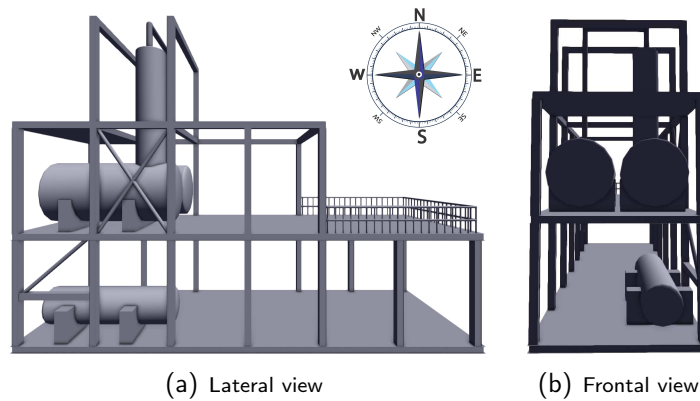


Figure 4.1: Geometry model and wind direction scheme for a semi-confined module

4.4.2 Leak Conditions

Initial calculations of leak temperature, leak density, and leak velocity were performed. It has been assumed an isentropic expansion in which the temperature and associated specific mass were calculated based on the local Mach number as follows:

- Leak temperature

By using the reservoir temperature as reference, the leak temperature was defined as:

$$\frac{T_{hole}}{T_{ref}} = \left(1 + \frac{C_p}{C_v} - 1 M^2 \right)^{-1} \quad (4.19)$$

$$T_{hole} = T_{ref} \left(1 + \frac{C_p}{C_v} - 1 M^2 \right)^{-1} \quad (4.20)$$

where the Mach number is $M = V/a$ and $a = \sqrt{\frac{C_p}{C_v}RT}$

- Leak density

Based on the value of T_{hole} , there is a ρ_{ref} resulting from the gas ideal equation of state.

$$\rho_{ref} = \frac{(P)(MM)}{R(T_{hole}(K))} \quad (4.21)$$

Now, for the leak density, the ρ_{ref} is replaced into the equation 4.22

$$\rho = \rho_{ref} \left(1 + \frac{\frac{C_p}{C_v} - 1}{2} M^2 \right)^{\frac{-1}{\frac{C_p}{C_v} - 1}} \quad (4.22)$$

- Leak velocity

The leak velocity (equation 4.23) takes into account the T_{hole} and the Mach number assumed.

$$V = \left(\sqrt{\frac{\frac{C_p}{C_v} R}{MM} (T_{hole}(K))} \right) M \quad (4.23)$$

- Leak position

For all the dispersion simulations, the methane release was positioned at the coordinate (12, -6, 2), as shown in Figure 4.2a. For changes in the leak direction, it was followed by the arrangement illustrated in Figure 4.2b.

In order to ensure that the wind velocity profile achieves the steady-state in the computational domain before the methane release begins, the leak started after 15 s of simulation, and it had a duration of 215 s.

4.4.3 Scenarios Outline for Dispersion simulations

The dispersion simulations were conducted to evaluate the influence of key parameters in the cloud volume. The parameters were the leak rate, leak direction, wind speed, wind density and wind direction.

The dispersion scenarios were defined by considering eight wind directions: North, South, East, West, North-West, North-East, South-East and South-West (see Figure 4.1); and

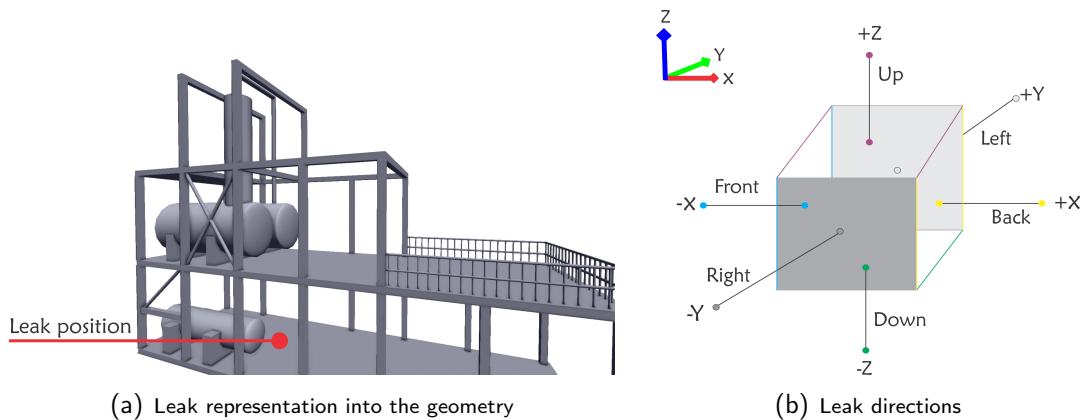


Figure 4.2: Leak position and directions represented into the geometry

Table 4.1: Group distribution for the dispersion simulations

Group Distribution and Variations				
Group	Parameters fixed			Parameters varied
First set	1A	up leak direction	6 m/s wind speed and 50 kg/s leak rate	Wind direction
	1B		50 kg/s leak rate and west wind direction	Wind speed
	2A	west wind direction and up leak direction	3 m/s wind speed	Leak rate
	2B		6 m/s wind speed	
	3A	6 m/s wind speed and west wind direction	50 kg/s leak rate	Leak direction
	3B		100 kg/s leak rate	
Second set	4A	5 kg/s leak rate and up leak direction	2 m/s wind speed	Wind direction
	4B		6 m/s wind speed	
	4C		8 m/s wind speed	
	5A	25 kg/s leak rate and up leak direction	2 m/s wind speed	
	5B		6 m/s wind speed	
	5C		8 m/s wind speed	
	6A	200 kg/s leak rate and up leak direction	2 m/s wind speed	
	6B		6 m/s wind speed	
	6C		8 m/s wind speed	
Third set	7A	50 kg/s leak rate and up leak direction	2 m/s wind speed	
	7B		6 m/s wind speed	
	7C		8 m/s wind speed	
	8A	100 kg/s leak rate and up leak direction	2 m/s wind speed	
	8B		6 m/s wind speed	
	8C		8 m/s wind speed	
Fourth set	9A	6 m/s wind speed and 50 kg/s leak rate	front leak direction	
	9B		up leak direction	
	9C		back leak direction	
	9D		left leak direction	
	9E		right leak direction	
	9F		down leak direction	

six leak directions: up, down, front, back, right, and left (see Figure 4.2). Different values of leak rate ranging from 0.5 to 500 kg/s and wind speed ranging from 1 to 12 m/s were evaluated. These values were defined based on the HSE offshore release report (HSE, 2001), and the dispersion scenarios were organized within a dispersion control (refers to Table 4.1).

4.4.4 Simulations Setting Up in FLACS

To setup the simulations into the CFD package in FLACS, it was necessary to perform initial calculations of leak area, leak cell width, leak cell length, and turbulence length scale. These calculations are described below:

Leak area

$$A_{leak}(m^2) = \frac{\dot{q}}{u_{leak}\rho_{leak}} \quad (4.24)$$

Leak cell width

$$LCW(m) = \sqrt{A_{leak}} \quad (4.25)$$

Leak cell length

$$LCL(m) = (LCW)(1.9) \quad (4.26)$$

Turbulence length scale

$$l = (0.2)(2)\sqrt{\frac{A_{leak}}{\pi}} = 0.2D \quad (4.27)$$

In the leak cell length calculation, a factor of 1.9 out of 2 was used based on Gexcon (2018) guidelines to ensure that the gas release will occur under a subsonic condition. In equation 4.27, D is the nozzle diameter, and the estimations of turbulence length scale parameter should be around 10% to 20% of the nozzle diameter (GEXCON, 2018).

Meshing Design

Given the geometry dimensions, the computational domain was set as twice the length in each direction, except for z-direction, where the computational domain is 1.5 the height of the geometry. The dimensions of the computational domain were set to assure the stability and robustness of the solution.

The computational domain can be found in Figure 4.3. For all cases, a fixed grid line was set in between the decks, at each boundary of the deck. This procedure ensures that the final mesh does not have gaps in the geometry affecting the porosity calculation (GEXCON, 2018). For the mesh design, a CFD-FLACS mesh inflation procedure was considered. Based on the different values of leak rate 17 sizes of mesh were built. Two of them, the finest (leak rate of 0.5 kg/s) and the coarsest mesh (leak rate of 500 kg/s), are illustrated in Figure 4.3.

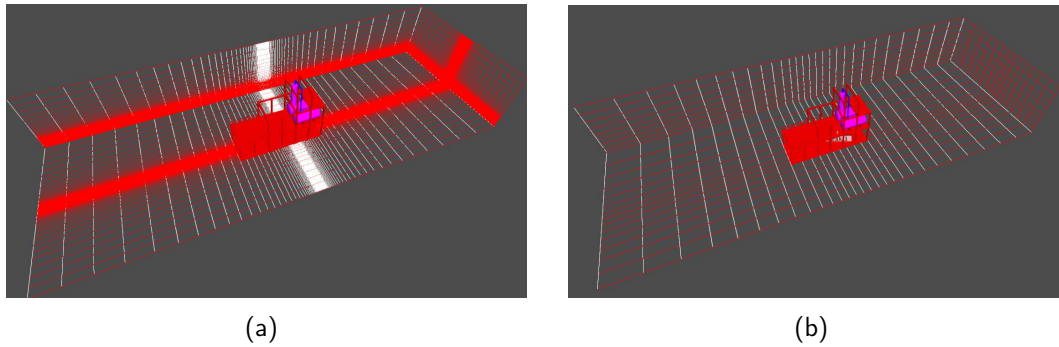


Figure 4.3: Geometry meshing for two different leak rates: (a) 0.5 kg/s of leak rate, (b) 500 kg/s of leak rate.

The grid in the region near the leak was built based on the cell length of the leak patch, calculated in section 4.4.4.

In the direction of the leak, a fixed grid line was set 5 m ahead of the patch. Uniform mesh spacing 1 m was set in this direction, then the mesh is stretched by a factor of 20% applied to the leak cell dimension. In this last step, the mesh is stretched until the end of the computational domain. Details of the mesh refinement are also shown in Figure 4.3.

The CFL number ranged from 20 to 40 in accordance with the mesh. The wind boundary conditions were set as prescribed velocity while the outflow boundary conditions were modeled based on the nozzle equations.

In all simulations, the turbulence intensity was set as 10%, and the length scale reflected the hole size in each case. The Pasquill class was moderate stable.

4.5 Dimensional Analysis

The dimensional analysis is a technique that helps in having a physical and engineered insight of a phenomenon by grouping all the significant parameters that represent it. This type of analysis describes some behavior of fluid flows obtaining analytical descriptions of the phenomena under study (FOX *et al.*, 2009).

This work uses the Buckingham Pi theorem to perform the dimensional analysis. The theorem is a formal method which states that n variables and parameters have a relationship to the form (KUNDU; COHEN, 2002):

$$f(p_1, p_2, \dots, p_n) = 0 \quad (4.28)$$

Where p are variables involved in the problem. Firstly, a set of independent variables influencing the dependent variable needs to be identified. Those n variables can be combined to form $(n - r)$ dimensionless groups. The rank is represented by r and n are the total number of variables. The functional equation is written as (KUNDU; COHEN, 2002):

$$\Pi_1 = \varphi(\Pi_2, \Pi_3, \dots, \Pi_{n-r}) \quad (4.29)$$

Five main steps must be followed to apply this theorem:

- Step 1: select variables and parameters
- Step 2: create the dimensional matrix
- Step 3: rank the dimensional matrix
- Step 4: determine the number of dimensionless groups
- Step 5: formulate the dimensionless group

The theorem was used to define a dimensionless flammable cloud (\hat{V}) based on the main variables that influence the gas dispersion of flammable material.

In the following section, the theorem is applied with two approaches: Firstly, a dimensional analysis by considering four factors (leak rate, density, wind speed, and flammable cloud volume). The second approach considered an additional parameter, namely the characteristic length (squared) of the geometry under investigation.

4.6 Application of the Buckingham Pi Theorem for Gas Dispersion

4.6.1 Dimensional Analysis without the Geometry Effects

The dispersion analysis evaluation led to the definition of the flammable volume as function of five main variables, so:

$$V = f(\dot{q}, u, \rho, \theta, \beta) \quad (4.30)$$

Where V is the cloud volume, \dot{q} is the leak rate, u wind speed, ρ fluid density, θ leak direction, and β wind direction.

The development of a dimensionless cloud volume \hat{V} began with the coupling of the affecting parameters using the Buckingham Pi theorem as presented in the following steps:

Selecting variables and parameters The variable V_f , defined as the flammable gas volume, is unknown, and it is named as the solution variable. The solution variable is V_f were coupled with the independent variables flow density (ρ), leak rate (\dot{q}), and wind speed (u) to form a variable set. Parameters related to leak and wind direction were not considered part of the dimensional analysis because they cannot be dimensionless. Therefore, the resulting functional dependence between parameters is:

$$f(V_f, \dot{q}, u, \rho) = 0 \quad (4.31)$$

$$V_f = f(\dot{q}, u, \rho)$$

Creating the dimensional matrix The four variables can be presented in terms of basic dimensions, such as mass (M), time (T), and length (L). In that way, the dimensional matrix is created by listing the dimensions.

	V_f	\dot{q}	u	ρ
M	0	1	0	1
L	3	0	1	-3
T	0	-1	-1	0

Ranking the matrix The rank of a matrix was defined by the size of the largest square submatrix with nonzero determinants. For the matrix obtained, the rank was 3.

Determining the dimensionless groups By using $(n - r)$, where n is the total number of variables and r is the dimensional matrix's rank. With a rank of 3 and n equal to 4, we have one dimensionless group.

Formulating the dimensionless group By employing algebra, r parameters were selected from the dimensional matrix (repeating parameters). These parameters enclosed the dimensions M, T, and L.

The standard dimensional analysis leads to the following dimensionless group:

$$\Pi_1 = u^a \rho^b \dot{q}^c V_f \quad (4.32)$$

$$M^0 L^0 T^0 = \left(\frac{L}{T}\right)^a \left(\frac{M}{L^3}\right)^b \left(\frac{M}{T}\right)^c L^3 \quad (4.33)$$

$$M \rightarrow 0 = b + c, L \rightarrow 0 = a - 3b + 3, T \rightarrow 0 = -a - c$$

$$a = 3/2; b = 3/2; c = -3/2$$

Replacing the values calculated,

$$\Pi_1 = \frac{u^{3/2} \rho^{3/2} V_f}{\dot{q}^{3/2}} \quad (4.34)$$

Equation 4.34 called \hat{V} describes the dispersion phenomena by relating the gas convective flow with the momentum of the leak release. Here, the V_f is equivalent to the Q9 output in FLACS (refer to \hat{V} calculations in Appendix A for more information).

4.6.2 Dimensional Analysis with the Geometry Effects

In this second approach, the dimensional analysis includes the effect of the geometry including the factors mentioned in Section 4.6.1. This analysis was used later for the definition of a second dimensionless number R.

Selecting variables and parameters The variable V_f is also defined as the flammable gas volume. This time, the solution variable is V_f , and the flow density (ρ), leak rate (\dot{q}), characteristic length per volume unit of the geometry (A), and wind speed (u) comprise the rest of the variable set.

The resulting functional dependence between parameters should be:

$$f(V_f, \dot{q}, u, \rho, A) = 0 \quad (4.35)$$

$$V_f = f(\dot{q}, u, \rho, A)$$

Creating the dimensional matrix The five variables can be presented in terms of basic dimensions, such as mass (M), time (T), and length (L). In that way, the dimensional matrix is created by listing the dimensions.

	V_f	\dot{q}	u	ρ	A
M	0	1	0	1	0
L	3	0	1	-3	-2
T	0	-1	-1	0	0

Ranking the matrix The rank of the matrix was 3.

Determining the dimensionless groups With a rank of 3 and n equal to 5, we have two dimensionless groups.

Formulating the dimensionless group For a given geometry (A) and a leak direction (θ), the standard dimensional analysis leads to the following dimensionless groups:

$$\Pi_1 = u^a \rho^b \dot{q}^c V_f \quad (4.36)$$

$$M^0 L^0 T^0 = \left(\frac{L}{T}\right)^a \left(\frac{M}{L^3}\right)^b \left(\frac{M}{T}\right)^c L^3 \quad (4.37)$$

$$M \rightarrow 0 = b + c, L \rightarrow 0 = a - 3b + 3, T \rightarrow 0 = -a - c$$

$$a = 3/2; b = 3/2; c = -3/2$$

Replacing the calculated values of a , b and c , the first dimensionless number is:

$$\Pi_1 = \frac{u^{3/2} \rho^{3/2} V_f}{\dot{q}^{3/2}} \quad (4.38)$$

Now, for the second dimensionless number, we have:

$$\Pi_2 = u^d \rho^e \dot{q}^f A \quad (4.39)$$

$$M^0 L^0 T^0 = \left(\frac{L}{T}\right)^d \left(\frac{M}{L^3}\right)^e \left(\frac{M}{T}\right)^f L^{-2} \quad (4.40)$$

$$M \rightarrow 0 = e + f, L \rightarrow 0 = d - 3e - 2, T \rightarrow 0 = -d - f$$

$$d = 1; e = -1; f = -1$$

Replacing the calculated values of d, e and f, the second dimensionless number is:

$$\Pi_2 = \frac{\dot{q}}{\rho VA} \quad (4.41)$$

The dimensional analysis led to two dimensionless quantities, and they are described as:

1. Π_1 relates the gas convective gas flow with the momentum of the leak release
2. Π_2 represent the relationship of the leak rate with the airflow within a specific area or the dimensionless leak rate

Chapter5

Numerical Results and Modeling

5.1 Introduction

This chapter presents the numerical results obtained after a systematic evaluation of different sets of dispersion scenarios described in Chapter 4. Analysis of the results of these sets are presented, and the Buckingham Pi theorem is used to calculate a dimensionless flammable cloud volume.

The influence of the wake volume for a proposed model is evaluated in the application of the Pi theorem. Lastly, based on proposed model results, a more robust model for flammable cloud volume calculation was developed by considering the geometry effects. This chapter shows the statistical analysis, validation and applications of the proposed models.

5.2 Numerical Simulations of Dispersion Scenarios

As described in Table 4.1, the dispersion scenarios were divided into four sets according to the specification of leak rate, wind speed and leak direction. The first set comprises scenarios from group 1A to group 3B. The second set includes data from group 4A to group 6C. The third set addresses findings from group 7A to group 8C and the last set includes numerical calculations from group 9A to group 9F.

All of these scenarios were simulated and the CFD-FLACS stoichiometric cloud volume (Q_9) was obtained for each one. The analysis of each set is described below and for illustration purposes, the largest clouds of the first set of scenarios are shown in Appendix A.

Figure 5.1 presents the numerical results provided by the simulations from groups 1A to 3B (Please, refer to Table 4.1).

The largest flammable cloud was obtained for the following configuration: leak rate of 50 kg/s , wind speed of 4 m/s , Up leak direction and West wind direction. The formation of this cloud was due to the module's re-circulation zone caused by the separation of the boundary layer from the large objects in the module (see the vessels in Figure 4.1).

For the dispersion conditions defined in groups 1A to 3B (refer to Table 4.1 and

Figure 5.1), the Up leak jet direction formed clouds with volumes around 1700 m^3 , while the rest of the leak jet directions had a maximum value near to 500 m^3 .

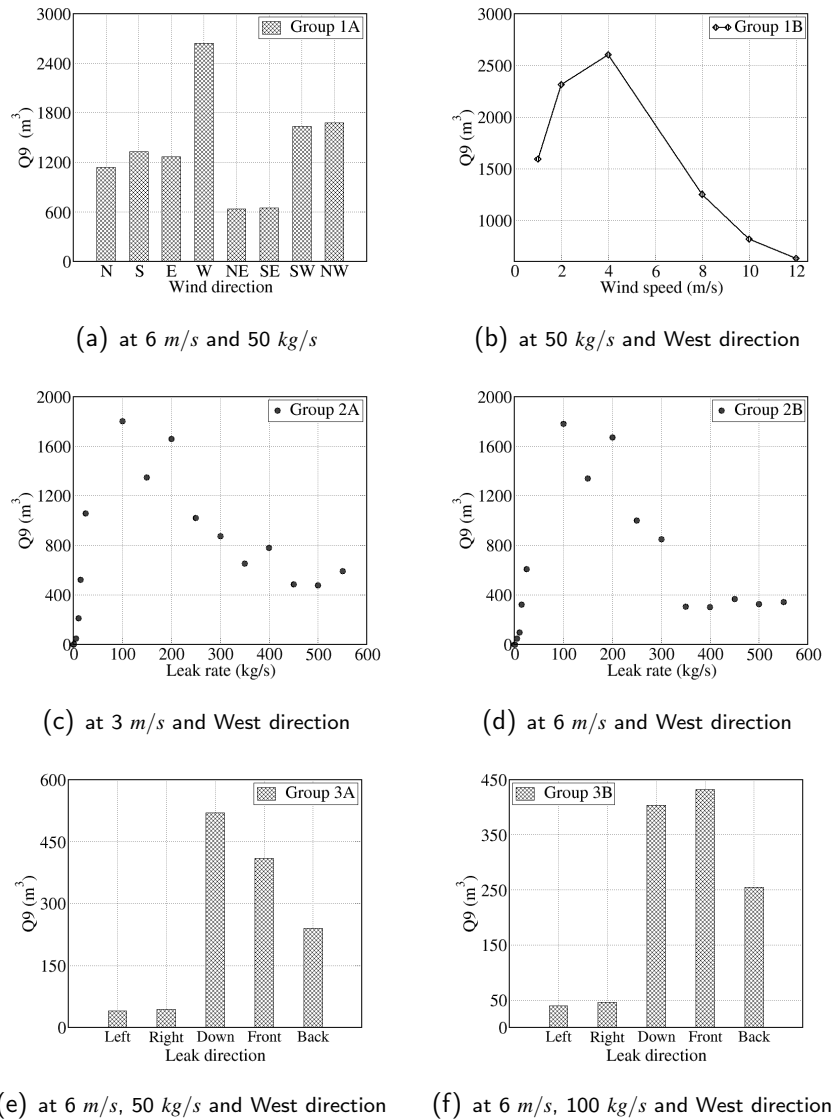


Figure 5.1: First set of dispersion scenarios: (a) variations of wind direction at up leak jet direction, (b) variations of wind speed at up leak jet direction, (c) and (d) variations of leak rate at up leak jet direction, (e) and (f) variations at different leak directions

Hence, to simplify the dispersion analysis and based on these examinations, the analysis turned narrower, and only the Up leak direction was used in the majority of the following scenarios.

From Figure 5.2 to Figure 5.5 the simulation results of groups 4A to 8C (refer to Table 4.1) are presented. These dispersion scenarios were set for three different values of wind speed (2 m/s , 6 m/s and 8 m/s), and four values of leak rate (25 kg/s , 50 kg/s , 100 kg/s and 200 kg/s) at fixed leak direction (Up) for all wind directions. Here, the main purpose was

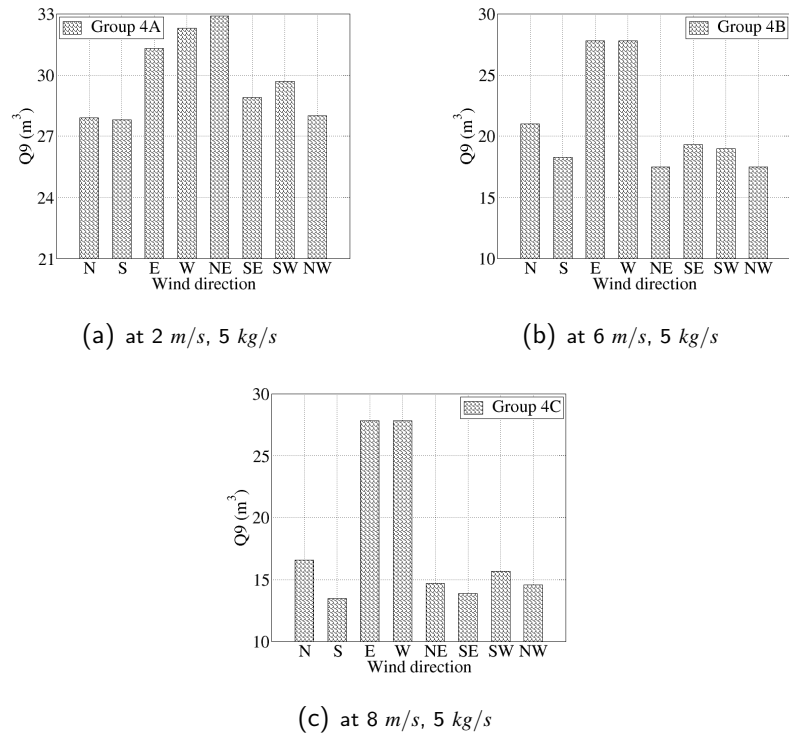


Figure 5.2: Second set of dispersion scenarios only considering variations of wind direction and three fixed values of wind speed of 2, 6 and 8 m/s: (a),(b) and (c) at fixed leak rate of 5 kg/s

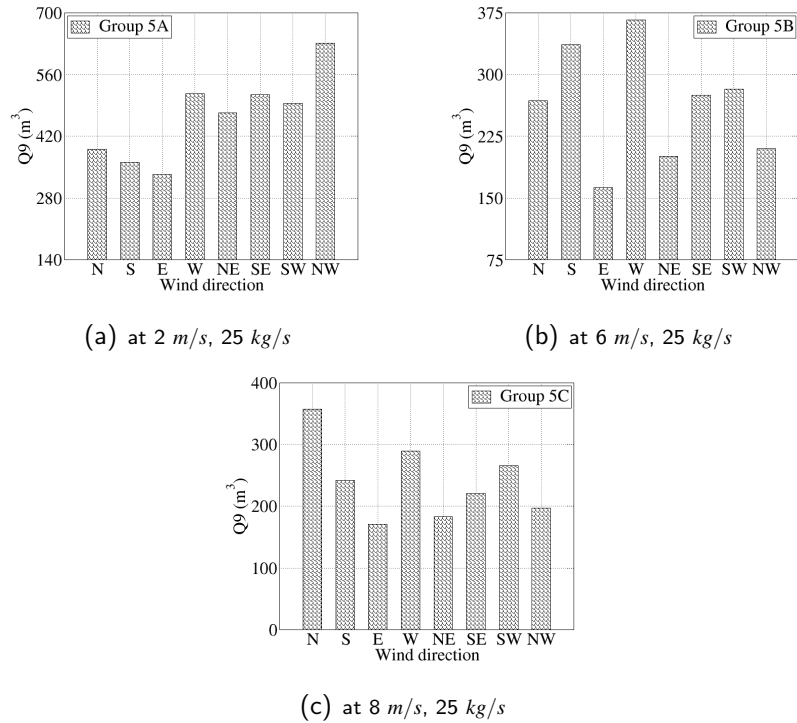


Figure 5.3: Second set of dispersion scenarios only considering variations of wind direction and three fixed values of wind speed of 2, 6 and 8 m/s: (a),(b) and (c) at fixed leak rate of 25 kg/s

to evaluate how the wind direction affected the Q9 value for certain conditions.

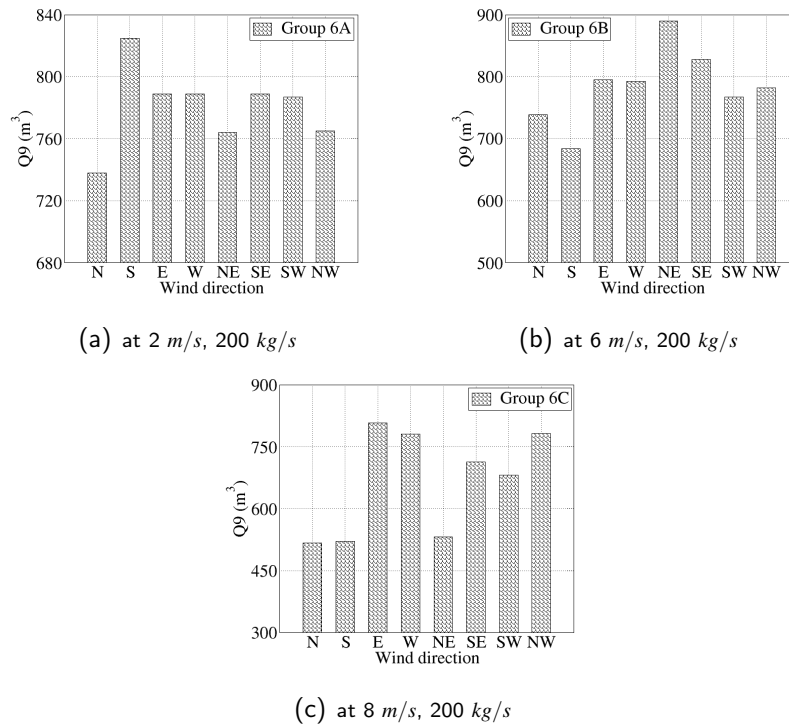


Figure 5.4: Second set of dispersion scenarios only considering variations of wind direction and three fixed values of wind speed of 2, 6 and 8 m/s : (a), (b) and (c) at fixed leak rate of 200 kg/s

In scenarios 4A to 4C (Figure 5.2a to Figure 5.2c), it is observed that the wind directions West and East presented the largest clouds. However, a large cloud volume is also presented at North-East wind direction for group 4A (wind speed equal to 2 m/s).

For groups 5A to 5C (Figure 5.3a to Figure 5.3c), it is observed a sinusoidal behavior when varying the wind direction. It is also verified that at lower values of wind speed, greater values of Q_9 were obtained. In these cases, the most affected directions were placed at West, South-East, and South-West.

Figure 5.4 presents the results provided by the dispersion scenarios of group 6. As observed for dispersion scenarios with leak rate of 5 kg/s (Figure 5.2) and 25 kg/s (Figure 5.3). A significant variation in the flammable volume when varying the wind direction was noticed.

For group 6A (Figure 5.4a), the South wind direction presented a large flammable gas cloud with a volume of 820 m^3 for wind speed of 2 m/s . However, when increasing the wind speed, different wind directions are responsible for the largest cloud volumes: North-East and South-East for wind speed of 6 m/s (Figure 5.3b) and the North-West, West, and East for wind speed of 8 m/s (Figure 5.4c).

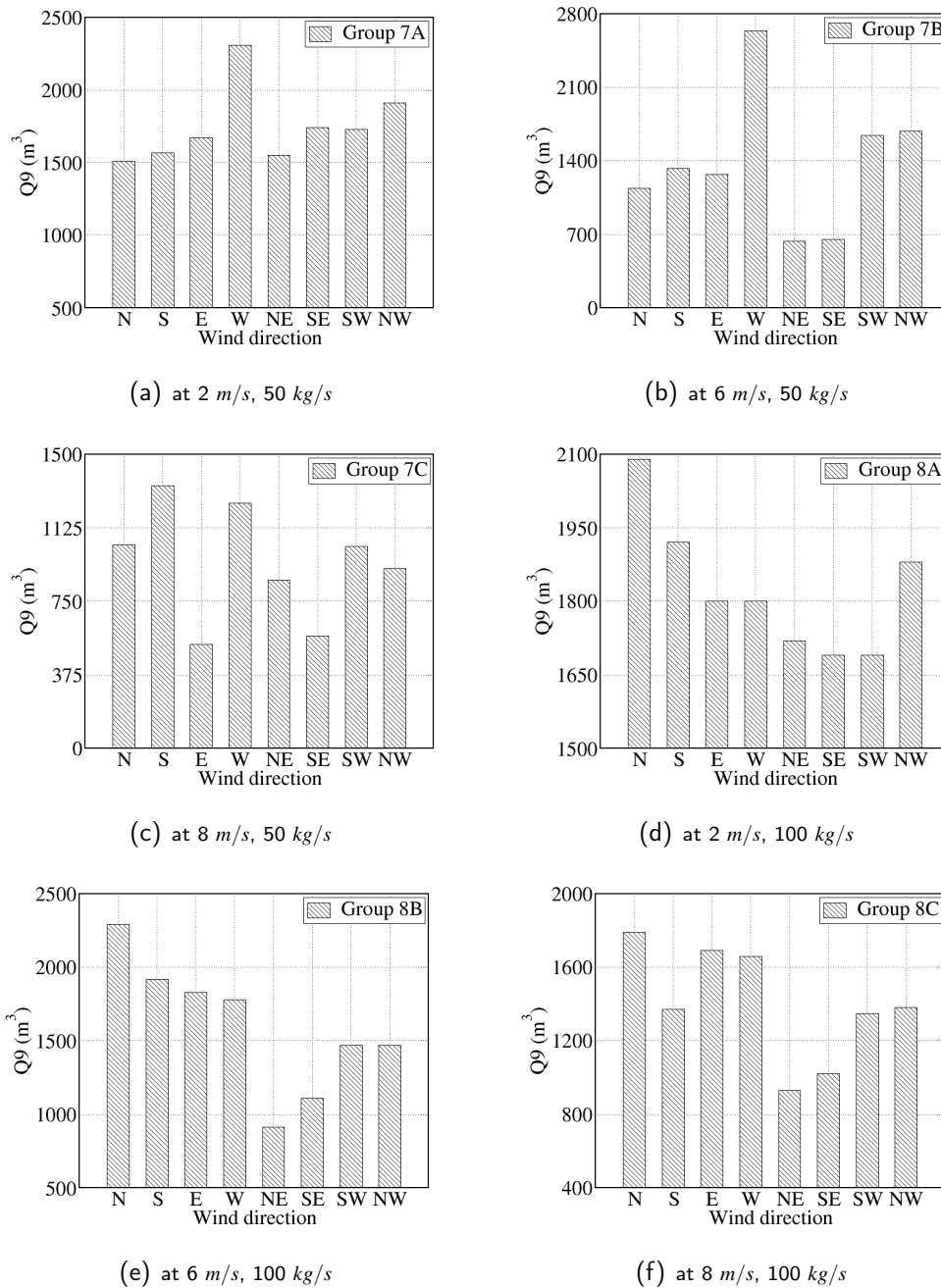


Figure 5.5: Third set of dispersion scenarios only considering variations of wind direction and three fixed values of wind speed of 2, 6 and 8 m/s : (a),(b) and (c) at fixed leak rate of 50 kg/s ; (d),(e) and (f) at fixed leak rate of 100 kg/s

Figure 5.5 shows six groups of scenarios that were performed for two leak rates (50 kg/s and 100 kg/s) based on the (Health and Safety Executive) report.

Considering the groups 7A and 7B (Figure 5.5a and Figure 5.5b), where the values of wind speed were set as 2 m/s to 6 m/s respectively, the West wind direction represented the worst scenario for cloud formation.

Likewise, when the wind speed increased to 8 m/s (Figure 5.5c), the formation of

larger flammable clouds was favored in the South direction. It can be explained by the fact that the wind tended to move the cloud near the location of the obstacles forming a large re-circulation zone.

For the group 8A to group 8C (Figure 5.5d to Figure 5.5f), it was identified a representative pattern in the North wind direction for all the scenarios. This behavior may be due to the relationship between the amount of material dispersed with the wind speed. As the wind speed increases, different directions, such as East and West also presented large values of flammable cloud (Figure 5.5f).

Subsequently to the extensive numerical analysis of different dispersion scenarios, and looking at the flammable cloud volume (Q9), it was remarked that the flammable volume relies on four main parameters: leak rate, leak direction, wind speed, and wind direction. To couple these four parameters in a single number, the Buckingham Pi Theorem was used.

5.3 Numerical Modeling

5.3.1 Flammable Cloud Volume Modeling: M-01

In order to evaluate the flammable cloud volume behavior, we proceeded to calculate the dimensionless volume (\hat{V}) for each set compiled in Table 4.1.

For the first set of dispersion scenarios, \hat{V} ranged from 0.16 to 61.87. For the second set from 0.53 to 62.28, the third set from 0.68 to 61.97, and the fourth from 0.68 to 61.87.

The values showed that the stoichiometric cloud flammable volume (Q9) is directly proportional to \hat{V} . However, when the leak rate is larger, \hat{V} decreased even for large values of Q9. An example of this behavior was observed for the scenario 7A where the highest value of \hat{V} was obtained at the South direction; and 2A where the lowest cloud was calculated at 500 kg/s of leak rate (refer to Appendix A for more information).

The results of groups 8B and 8C were plotted against wind direction as an example to understand the pattern of the flammable cloud (Figure 5.6). It was observed that, for both groups, \hat{V} presented an oscillatory waveform, and then a slightly exponential behavior when varying the wind direction.

In order to simplify the complexity of the analysis, a dispersion model was proposed based on the oscillatory behavior showed in Figure 5.6.

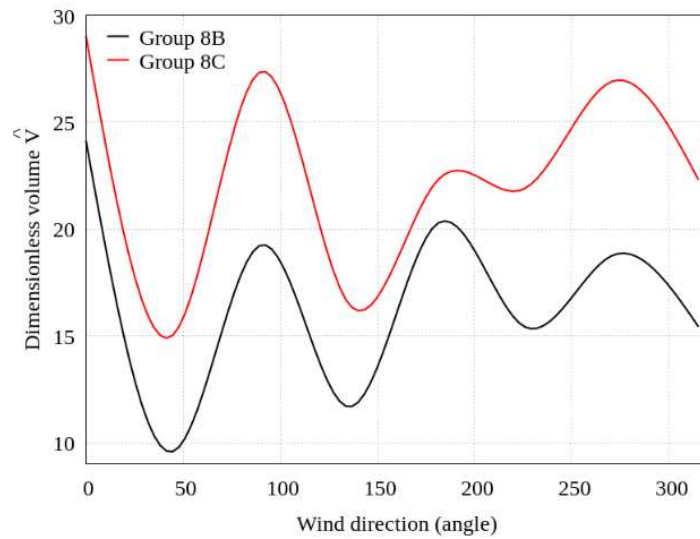


Figure 5.6: Representation of the waveform of the cloud volume based on the dimensional analysis for groups 8B and 8C (refer to Table 4.1)

A new set of dispersion scenarios (the fourth set showed in Table 4.1) was performed for the M-01 model's development. This group was named group 9 (50 kg/s , 6 m/s). The simulations considered six leak directions (front, back, up, down, left, right) and eight wind direction (N, S, SE, NE, SW, NW, W, E), giving a total amount of 48 simulations.

Values of \hat{V} were obtained for all scenarios and a model based on empirical insight was proposed following the procedure below:

1. Definition of two functions able to model the waveform and exponential pattern (as cosine and exponential functions)
2. Identification of the worst-case scenarios in group 9 useful for model's tuning
3. Specification of the wake conditions (wake angle and wake volume) for each scenario in group 9
4. Assign an amplitude and a mean
5. Assume two adjustable variables A and B to adjust the model
6. Solve the non-linear equation

The resulting mathematical, model called "**M-01**" model, is:

$$\hat{V}(\beta, \alpha) = \varepsilon + \delta \cos(A\beta) + V_w \exp[-B(\beta - \alpha)^2] \quad (5.1)$$

Where ε is the mean value, δ the amplitude, β the wind direction angle, V_w the wake volume, α the wake angle, and A, B are two tuning variables for each leak direction based on CFD data.

According to Equation 5.1, the proposed model presents two main parts: a sinusoidal function associated with the wind angle (direction); and an exponential part that accounts the quick rise of the cloud volume.

The M-01 model was developed based on the trigonometric circle and the associated sine-cosine relation, which resembles the wind direction as expressed by the wind rose.

The model was adjusted based on the worst-case scenarios (largest clouds) of group 9, summarized in Table 5.1 below:

Table 5.1: Worst-case scenarios of group 9 at different wind directions for each leak direction (50 kg/s of leak rate and 6 m/s of wind speed)

Leak direction	Wake angle	Q9 (m^3)	\hat{V}
Up	West	2080	61.87
Back	East	511	15.20
Left	North-East	77.9	2.32
Right	South	690	20.52
Down	East	660	19.63
Front	West	416	12.37

Figure 5.7 shows how the model adjusts with numerical data. The dimensionless volume (\hat{V}) was plotted against the wind direction (wind angle) for each leak direction.

In all graphs, the solid line shows the proposed M-01 mathematical model and the dots represent the CFD data. There is a notable agreement between the proposed model and the CFD findings.

The waveform shape and exponential form are verified for all cases. Therefore, the proposed model helps to understand the dispersion phenomena by considering the influence of the leak rate, wind speed, and wind direction.

Figure 5.8 shows how the M-01 model compares with CFD data within a factor of 2. The scatter was based on the results presented in Figure 5.7. The solid line indicates that the predicted (CFD data) and calculated (M-01 model) results are the same.

Analysis of Figures 5.7 and 5.8 indicates that the dispersion phenomena may be modeled by Equation 5.1 and be applied to real scenarios as CFD simulation does. An engineering procedure to guide the use of this M-01 model was described in Appendix C.

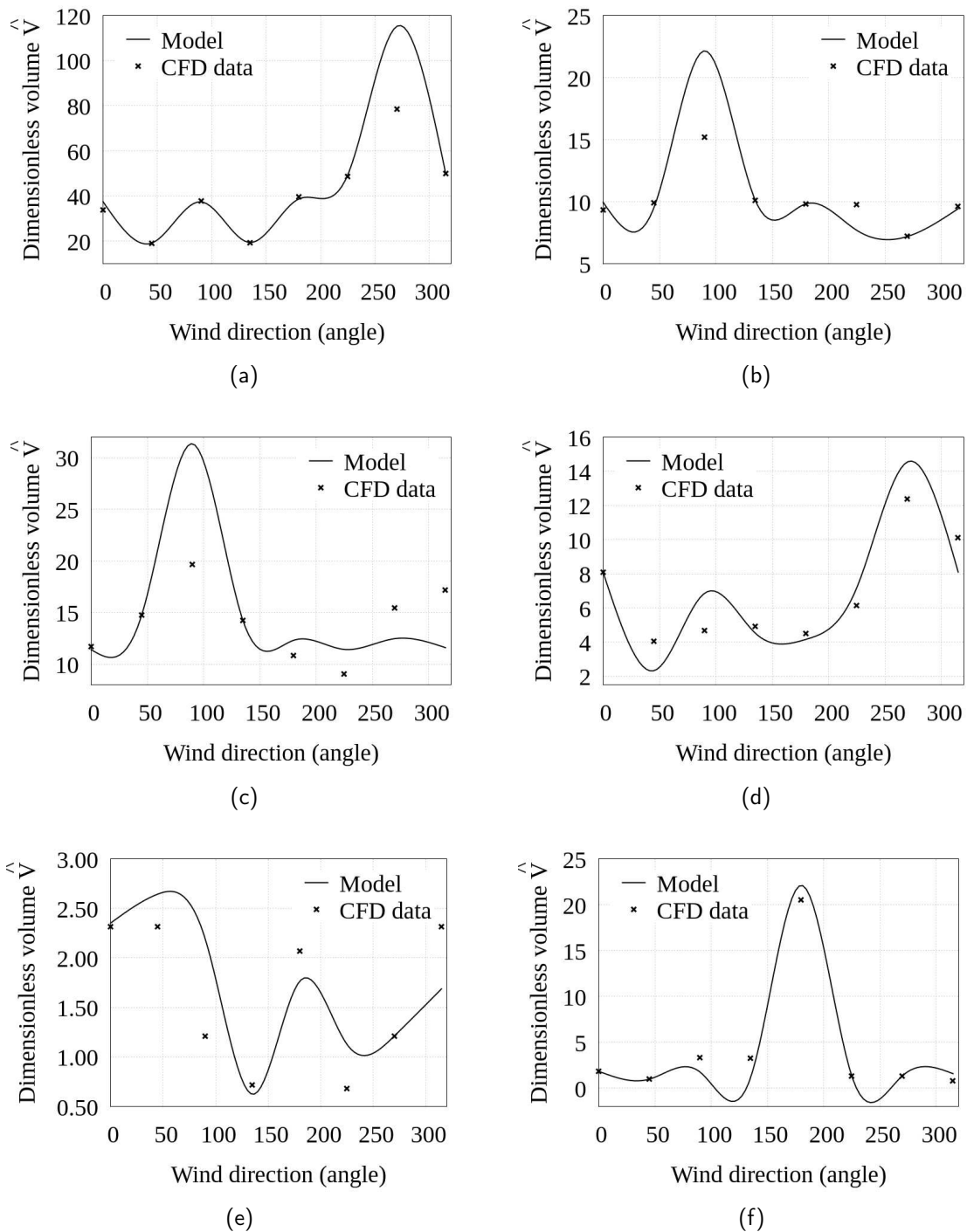


Figure 5.7: Comparison of CFD-data based on dimensional analysis with the mathematical model in the determination of \hat{V} at different leak jet direction: (a) Up leak jet direction, (b) Back leak jet direction, (c) Down leak jet direction, (d) Front leak jet direction, (e) Left leak jet direction, (f) Right leak jet direction.

The Influence of the Wake Volume in the M-01 Model

The M-01 model (equation 5.1) presents in its formulation two important variables: wake angle (α) and wake volume (V_w). This wake angle is defined as the angle that generates

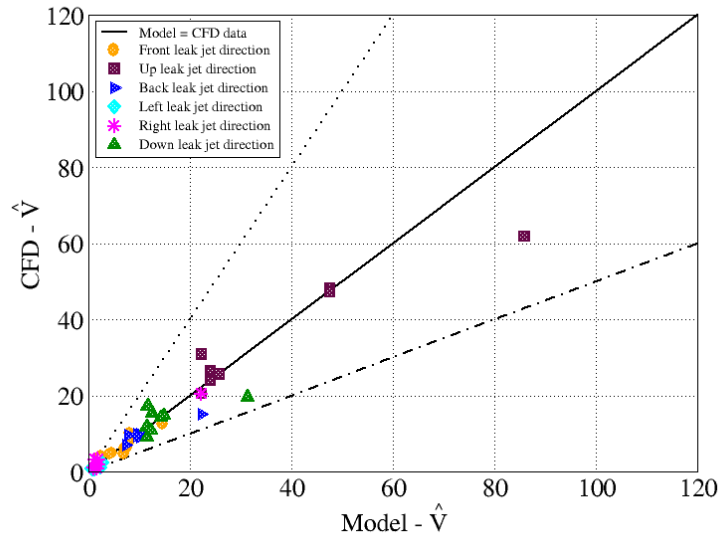


Figure 5.8: Analysis of the dimensionless volume obtained by CFD data and the values provided by the proposed mathematical model

large re-circulation zones in the wake of a bluff body. As a result, the size of the large flammable clouds obtained in dispersion scenarios with wind blowing from the wake angle, are called wake volume. In this sense, it is expected that each process area in the module presents a single wake wind responsible for the formation of the largest flammable cloud.

When analyzing the worst-case scenarios provided in Table 5.1, it was observed that the largest flammable volumes are obtained due to a combination of wind direction and leak direction. Thus, the wake angle may vary depending on the leak direction. This behavior can be explained by the presence of obstacles inside the geometry's model used in this study (Figure 4.1) and their interaction with the leak direction.

Although it was observed that the formation of large flammable clouds relies on the relationship between wind and leak direction, the up leak direction showed the highest value of \hat{V} among all the cases. Hence, based on this analysis, two approaches were defined for additional evaluation of the flammable cloud volume respect to the wake angle:

1. Same wake angle, different wind speeds and wind directions, and at up leak direction
2. Different wake angle, different wind speeds and wind directions, and at up leak direction

In the analysis, five groups were considered and named as $G4_5$, $G5_25$, $G7_50$, $G8_100$, $G6_200$. They are identified as GX_Y , where GX is the group, and Y is the leak

rate. These scenarios were simulated at three wind speeds (2, 6, and 8 m/s) and Up leak direction. Values of \hat{V} were calculated by using the M-01 model.

The first approach assumed calculations with the same wake angle for all wind directions, three wind speeds, and at Up leak direction. The second was set based on different wake angles obtained by the CFD results at the same leak and wind conditions. Both were performed to work out whether the variations of wake angle will influence in the model accuracy.

For instance, for a group of scenarios named G4_5, the $\hat{V}(\beta, \alpha)$ was obtained with the M-01 model and \hat{V} with the CFD data. Hence, calculations of dimensionless volume with the model and CFD were compared by calculating the absolute error.

The Table 5.2 compiled the sum of the absolute errors calculated for the scenarios used in the model development.

Table 5.2: Sum of absolute errors in the analysis of wake angle variations at up leak direction, different wind speeds and wind directions for a set of scenarios

Analysis of wake angle variations						
Case	Different wake angles			Same wake angle (270°)		
	Wind speed (m/s)					
	2	6	8	2	6	8
G4_5	153.00	83.06	82.35	152.80	83.06	82.35
G5_25	139.78	72.78	87.29	140.54	72.78	77.36
G6_200	181.87	168.00	160.38	18.81	167.34	162.20
G7_50	134.01	40.69	131.09	131.71	40.69	130.74
G8_100	162.99	85.43	56.44	162.43	85.71	69.96

It is seen that the sum of the absolute errors is closer between both approaches despite the wake angle varied with the wind direction. Thus, the assumption of having the same wake angle in dispersion analysis is valid from the engineering point of view.

Statistical Analysis of the M-01 Model

The performance and accuracy of the M-01 model were evaluated assuming fixed wake angle, which represented the worst-case scenario (west wind direction or 270 degrees).

The dispersion scenarios used were different from those chosen for the development of the model. Table 5.3 shows the configuration of the 120 dispersion scenarios used in this statistical analysis. Four main groups (group 4, group 5, group 7, and group 8) were addressed.

For each one of the groups, leak rates were set as: very small (5 kg/s), small (25 kg/s), medium (50 kg/s), large (100 kg/s) and very large (200 kg/s). Additionally, eight wind

directions and three wind speeds (2 m/s, 6 m/s, and 8 m/s) were considered.

Table 5.3: Group of scenarios used in the validation of the proposed model

Group	Parameters fixed*	Parameter varied
4A	5 kg/s leak rate	Wind direction
4B		
4C		
5A	25 kg/s leak rate	Wind direction
5B		
5C		
6A	200 kg/s leak rate	Wind direction
6B		
6C		
7A	50 kg/s leak rate	Wind direction
7B		
7C		
8A	100 kg/s leak rate	Wind direction
8B		
8C		

* Each parameter was evaluated at 2, 6, 8 m/s of wind speed and up leak direction

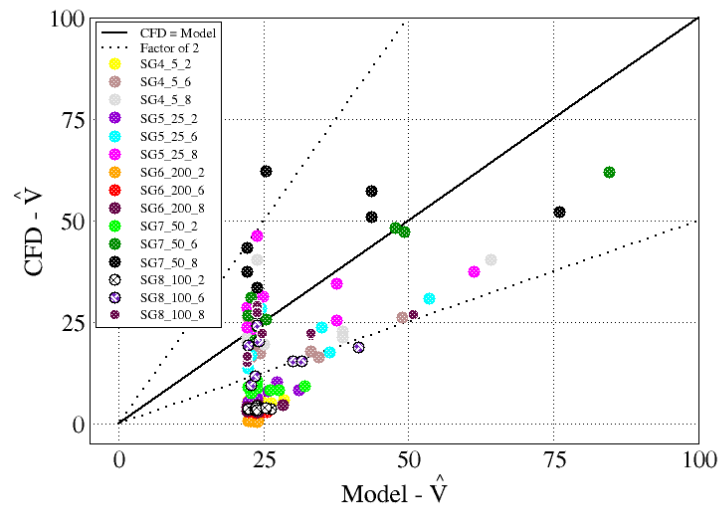


Figure 5.9: Accuracy evaluation and model validation of the 120 simulations

Figures 5.9 and 5.10 present the comparison between the values of \hat{V} obtained by CFD results and calculated by the M-01 model for all dispersion scenarios in Table 5.3.

The scenarios were identified as SGX_Y_Z: where S stands for "simulation"; G stands for "group", X stands for the group number, Y is the leak rate, and Z is the wind speed.

The solid line indicates that the predicted (CFD data) and calculated (M-01 model) results are the same, while the dashed lines represent a difference between the data within a factor of 2.

In both Figures 5.9 and 5.10, it was possible to observe that values of \hat{V} provided by the M-01 model are similar to those given by CFD simulation within the established interval. However, in some cases, the model is underestimating the dimensionless flammable volume. These cases are especially related to a very small wind speed value of 2 m/s and a very large leak rate of 200 kg/s (Figure 5.10).

Therefore, it is verified that the model works in a good agreement (good estimation of the cloud volume) with numerical simulations considering medium to large wind speeds and leak rates.

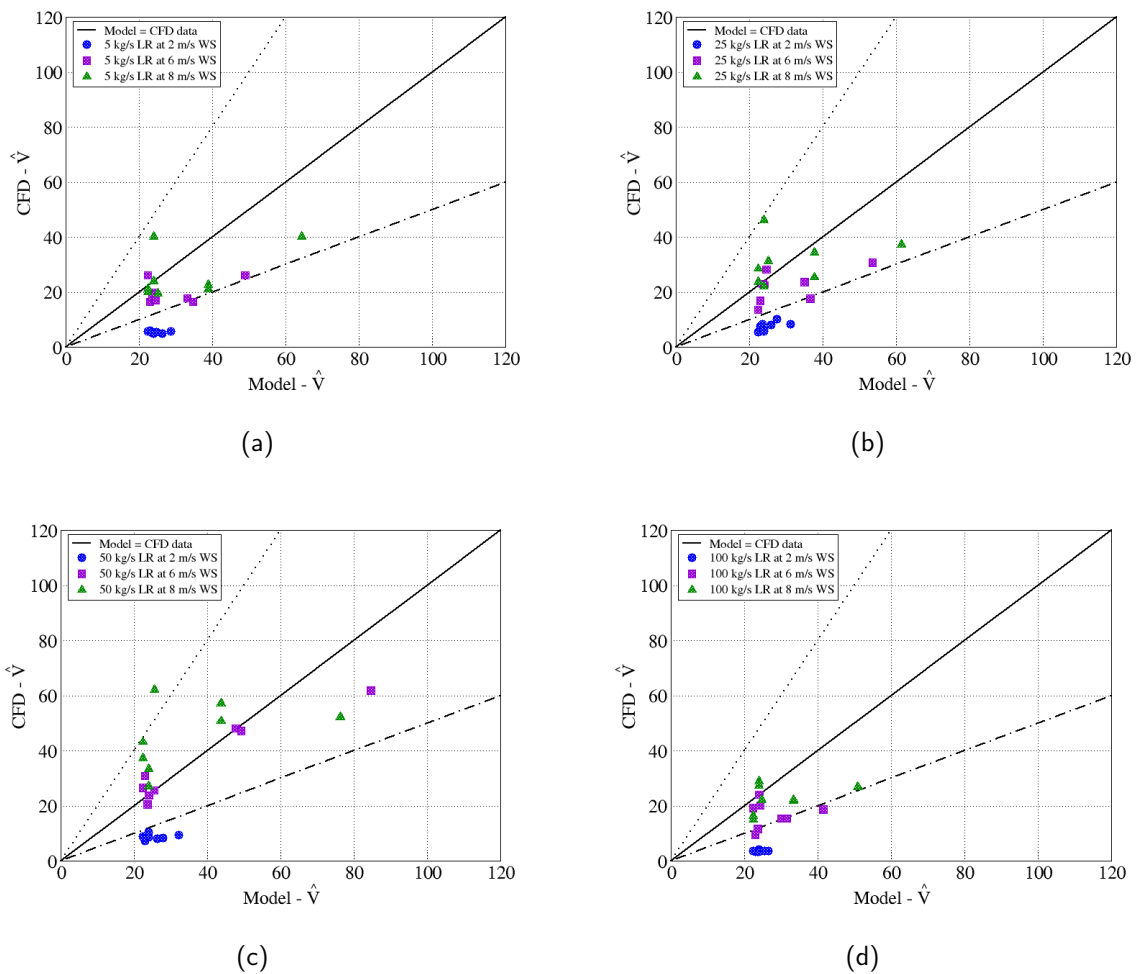


Figure 5.10: Accuracy evaluation and model validation against CFD data, and the model at different values of leak rate (LR) at 6 m/s and 8m/s of wind speed (WS): a) SG4_5, (b) SG5_25, (c) SG7_50, (d) SG8_100.

A complete statistical analysis of the M-01 model has been performed following the MEGGE protocol (MEGGE, 1997). In this protocol, the geometric mean and the variance are defined as:

1. Geometric Mean Bias (MG) = $\exp(\text{mean Ln}(P/O))$
2. Geometric Mean Variance (VG) = $\exp(\text{mean Ln}(P/O)^2)$

In the formulation above, P are the predicted values (Model) and O are the observed values (CFD data). Tables 5.4 and 5.5 presented a compilation of MG and VG values calculated for the dispersion scenarios used for the model validation.

The MG and VG values presented in these tables only considered values of 6 and 8 m/s for 5, 25, 50, and 100 kg/s, which represented the scenarios with the best agreement.

Another parameter for the statistical evaluation of the model is the FAC2 (fraction within a factor of two) value. According to the model evaluation protocol for HySEA (HISKEN *et al.*, 2016), values of FAC2 corresponds to the fraction of the data that satisfies $0.5 \leq \frac{X_p}{X_o} \leq 2$. This result provided a very good indication of the performance of the model. As observed in both Tables 5.4 and 5.5 the M-01 model agrees within the range indicated by the factor FAC2.

Table 5.4: Statistical performance and evaluation for groups with 6 m/s of wind speed at values of leak rate specified.

Case	MG	VG	FAC2
SG4_5	1.45	1.23	1.50
SG5_25	1.35	1.18	1.40
SG7_50	0.99	1.03	1.01
SG8_100	1.67	1.43	1.74

Table 5.5: Statistical performance and evaluation for groups with 8 m/s of wind speed at values of leak rate specified.

Case	MG	VG	FAC2
SG4_5	1.20	1.16	1.27
SG5_25	0.98	1.13	1.04
SG7_50	0.72	1.27	0.77
SG8_100	1.27	1.14	1.31

Figure 5.11 shows the geometric mean value (MG) plotted against geometric variance (VG). The solid vertical line represents zero variance, and the dashed lines represent the limits within a factor of 2.

Values of MG and VG that are equal to one implies "i" predictions 100% accurate. Likewise, values greater than 1 suggests under-prediction. The parabola defines the minimum value of VG for a given MG.

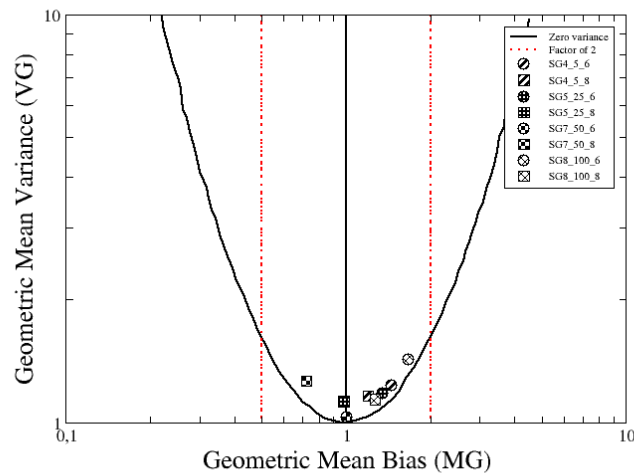


Figure 5.11: Geometric mean bias against geometric mean variance

By analyzing Figure 5.11, it was possible to verify that the M-01 model presents a good performance, providing a good agreement with CFD data for the calculation of the dimensionless flammable volume \hat{V} .

However, it is important to keep in mind that this first model was developed by considering only the four main parameters that influence the flammable volume (wind speed, leak rate, wind direction and leak direction). Thus, the effect of the geometry design of a process area in the flammable cloud formation was not included.

Therefore, in a second step of this work, a new mathematical model named **M-02** was developed to evaluate the geometric effects.

5.3.2 Numerical Analysis for the M-02 Model

The results obtained by the M-01 model presented significant underestimations for some environmental and leak conditions. In this sense, the development of a new model was necessary. The focus of this new model, called **M-02** model, was to consider the geometry effects, which were not included in the first M-01 model.

Initially, a new dimensional analysis was performed due to the inclusion of a new

parameter (characteristic length of the geometry, A) (refer to Section 4.6.2). Furthermore, numerical simulations were performed to evaluate specific dispersion scenarios, and finally, the M-02 model's validation took place.

The dimensionless number Π_1 was also found in this new dimensional analysis. This variable was called \hat{V} and represents a dimensionless cloud volume.

However, the number Π_2 is a new quantity, that appears in the calculations when the geometrical variable "A" was included. This new number was called R and represents the dimensionless leak rate.

The dimensional analysis performed in previous Section 4.6.2, suggested that the dispersion phenomena may be described by more than one single dimensionless number. In this sense, it is important to evaluate the relationship between the two dimensionless quantities and how they influence on the dispersion phenomenon.

For the development of the M-02 model, the dispersion scenarios were designed by keeping in mind that the flammable cloud formation can be described by the dimensionless numbers \hat{V} and R .

All simulation scenarios used for the first proposed model considered the Up leak direction. Additionally, 30 new simulations were performed for the remaining leak directions at the same leak rate and wind conditions. The new simulated scenarios consisted in: four wind speeds (2 m/s, 4 m/s, 6 m/s, and 10 m/s), one leak rate (50 kg/s), six leak directions (front, back, down, up, left, right), and one wind direction (west direction).

Overall, the numerical simulations performed for the development of the second model included two sets:

1. Fixed Up leak direction: five different leak rates (5, 25, 50, 100 and 200 kg/s), three different wind speeds (2, 6 and 8 m/s) at eight wind directions (N, S, E, W, SE, SW, NE, NW)
2. Fixed leak rate of 50 kg/s varying wind speed of 2, 6, 8 and 10 m/s considering west wind direction and the five remaining leak directions (front, left, right, down, and back)

For each set, the two dimensionless numbers \hat{V} and R were calculated. When these two quantities were plotted in a graph, an exponential pattern followed by a slight decay was observed (refer to Figure 5.12).

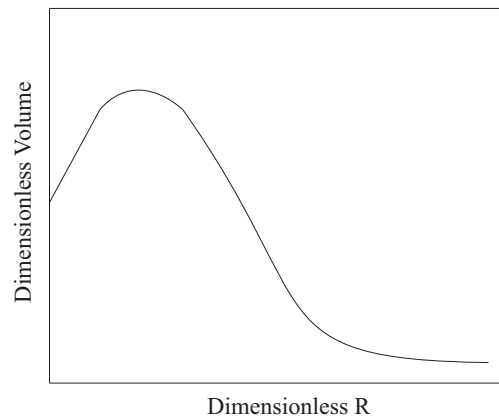


Figure 5.12: General representation of the flammable cloud behavior within the module after comparing the two dimensionless numbers

Figure 5.13 showed an example of this exponential behavior for the two sets of dispersion scenarios. It is possible to observe that values of R are smaller for 8 m/s (less than 0.06), while for 2 m/s of wind speed, they ranged from 0 to 0.25.

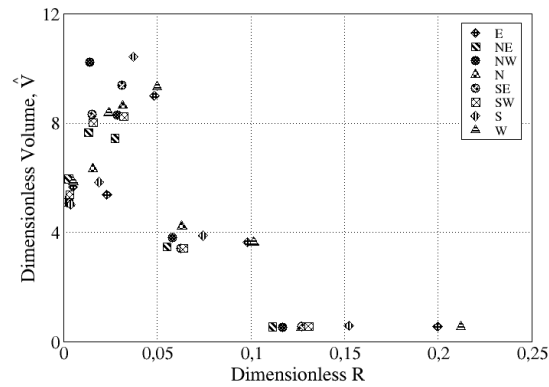
Moreover, the \hat{V} showed the opposite behavior, ranging with values around 70 as the wind speed increases. It was also verified that same values of R may be related to different values of \hat{V} , and the explanation of this fact is still under investigation.

The procedure applied for the development of the new M-02 model was:

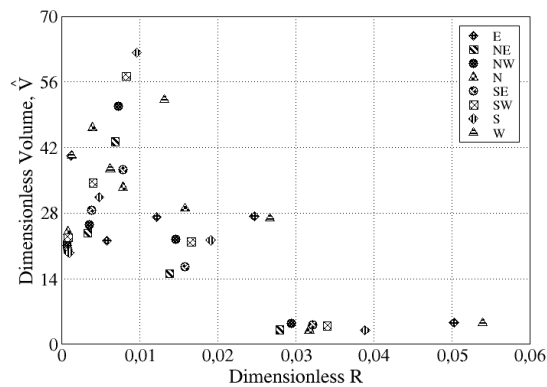
1. Identification of a mathematical function to model an exponential behavior
2. Assume two adjustable variables
3. Evaluate the ratio of the common variables between both dimensionless quantities and their relationship
4. Integrate all the variables into an equation, which is a function of R
5. Solve the equation

Based on this procedure, a new **M-02** physical model was proposed:

$$\hat{V}(R) = [A^2 \exp(-RB)]R^{\frac{3}{2}} \quad (5.2)$$



(a) 2 m/s



(b) 8 m/s

Figure 5.13: Comparison of the relationship of \hat{V} against R for two different wind speeds (2 m/s, and 8 m/s), five leak rates (5, 25, 50, 100, 200 kg/s), eight wind directions (N, S, E, W, SE, SW, NE, NW) and up leak direction

In the M-02 model, A and B are two adjustable variables that must be used to tuning the model considering the different wind and leak directions.

Figure 5.14 showed the model evaluation by tuning the variables A and B for different wind directions. It is observed that the values of $\hat{V}(R)$ calculated by the M-02 model tended to overestimate those results provided by CFD.

For East and South wind directions, all the numerical experiments are under the curve, while the West and North-east directions presented a slight underestimation.

The results presented in Figure 5.14 were compiled in a single graph (Figure 5.15). This graph shows an interesting behavior related to the cloud volume ($\hat{V}(R)$) values as long as the wind direction varies.

As long as the wind direction changed, the curves were plotted. The $\hat{V}(R)$ increases

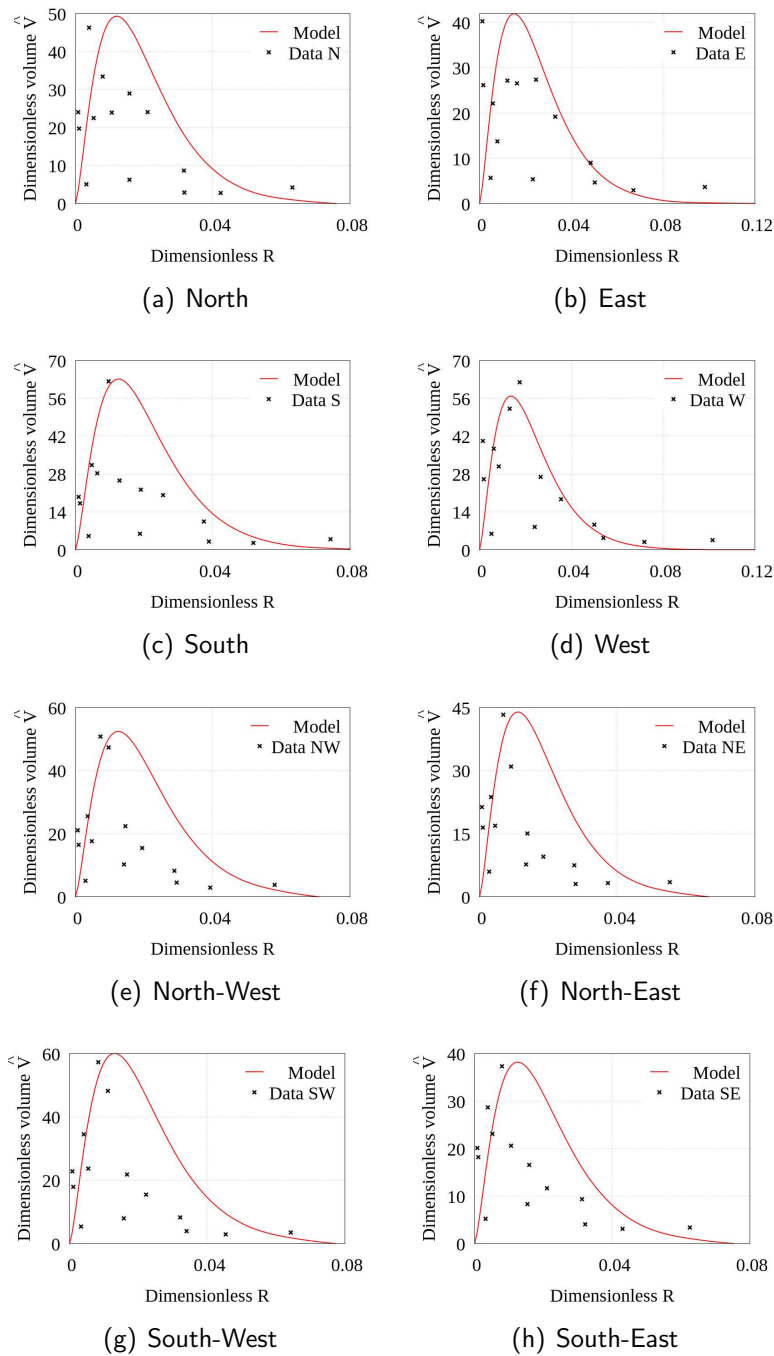


Figure 5.14: Comparison between $\hat{V}(R)$ model and R at different values of leak rate of 5, 25, 50, 100 and 200 kg/s at 2, 6 and 8m/s of wind speed considering the eight wind directions and at up leak direction.

by starting from South-East direction and finishing in South wind direction. This increase ranged from 38 to 64 of dimensionless volume, turning the compass rose completely.

In a second evaluation of the M-02 model, values of $\hat{V}(R)$ were compared with CFD data by adjusting the model parameters A and B according to different leak directions. The results of this analysis are illustrated in Figure 5.16.

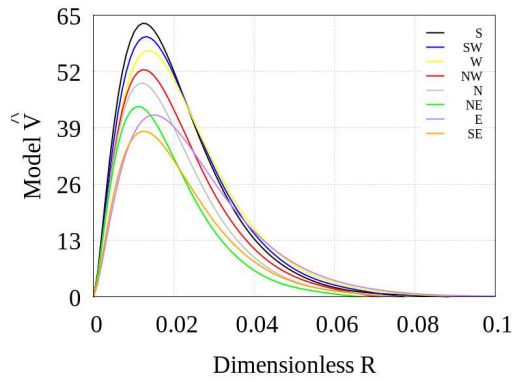


Figure 5.15: Compilation of data from Figure 5.14 of model $\hat{V}(R)$ against R for all the wind directions at up leak direction and 8 wind directions.

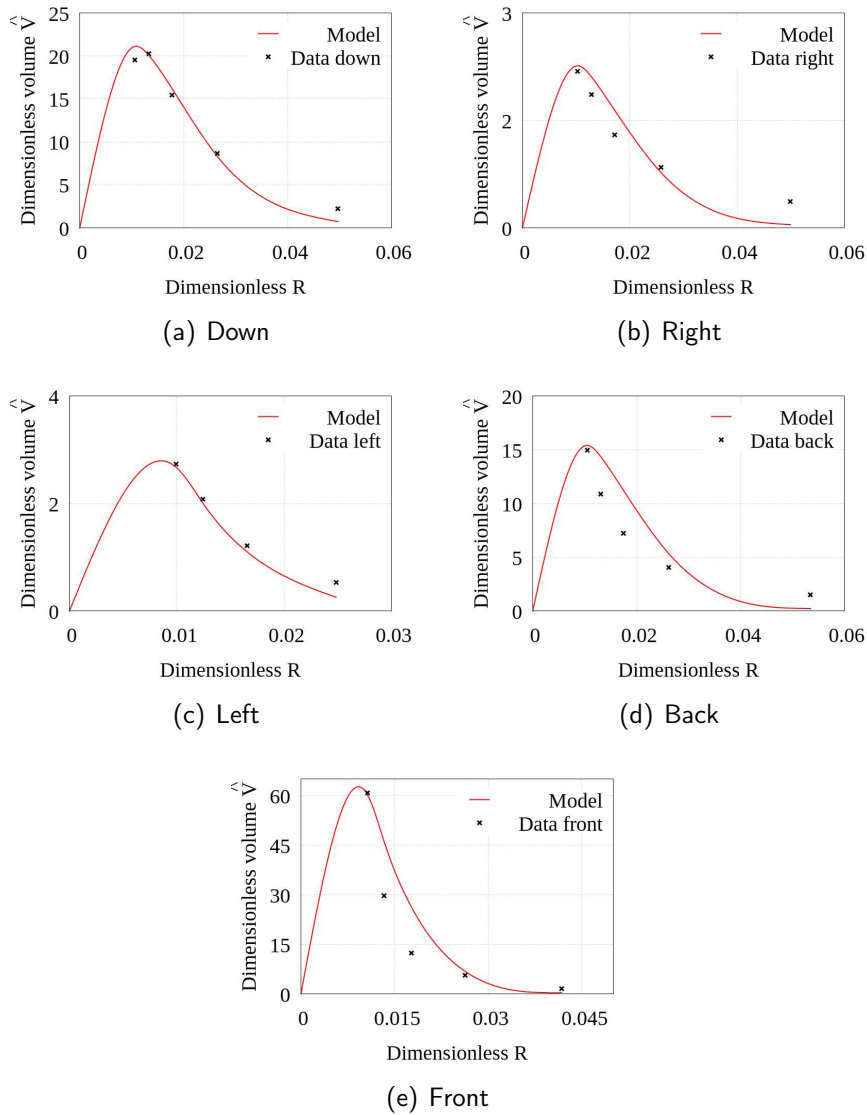


Figure 5.16: Comparison between $\hat{V}(R)$ model and R at fixed leak rate of 50 kg/s at 2, 6, 8 and 10 m/s of wind speed considering west wind directions at five leak directions (front, left, right, down, back).

Findings show the same exponential tendency of cloud volume, and the model represented perfectly the dynamics without outlasting the numerical experiments. Besides, in Figure 5.16, flammable clouds volumes with R values between 0.01 to 0.04 are well described by the model.

If we consider only Up leak direction (Figure 5.14), it was verified that for flammable cloud volumes with R ranging from 0.01 to 0.1 the M-02 model will also works in a good agreement with CFD data.

For both situations, the new proposed model presented a better fit for R ranging from 0.01 to 0.04, which comprises a wide amount of real potential dispersion scenarios.

Statistical Analysis and Validation of the New M-02 Model

For the model analysis and validation, a new set of dispersion scenarios were simulated in FLACS. Simulations were performed with R ranging from 0.01 to 0.1 to cover a wide range of scenarios.

The numerical simulations were defined by considering five values of leak rate (25, 48, 72, 95 and 120 kg/s) at fixed wind speed of 1.5 m/s for all wind directions, and up leak direction. Values of R were calculated by using the dimensionless number (R) and results are listed in Table 5.6.

Table 5.6: Values of R calculated based on a R_{ref} to obtain a specific leak rate for the validation analysis

R_{ref}	0.02	0.04	0.06	0.08	0.1
Leak rate	25	48	72	95	120
Wind direction	R Values				
N	0.02	0.04	0.06	0.08	0.10
S	0.03	0.05	0.07	0.09	0.12
E	0.03	0.06	0.09	0.12	0.16
W	0.04	0.07	0.10	0.13	0.17
NE	0.02	0.04	0.05	0.07	0.09
SE	0.02	0.04	0.06	0.08	0.10
SW	0.02	0.04	0.06	0.08	0.11
NW	0.02	0.04	0.06	0.07	0.09

A total amount of 40 dispersion scenarios were simulated and values of \hat{V} and $\hat{V}(R)$ by using the M-02 model were calculated.

Subsequently, the model was tuned by adjusting A and B values for each wind

direction as presented in Table 5.7.

Table 5.7: Values of adjustable variables (A and B) for model validation

Wind direction	Variables	
	A	B
N	80	50
S	90	50
E	62	33
W	72	35
NE	90	55
SE	90	52
SW	80	45
NW	86	55

Values of $\hat{V}(R)$ were plotted against \hat{V} , as shown in Figure 5.17. Findings showed that for all wind directions, the values of R around 0.02 and 0.1 gave over-predicted values of the dimensionless volume.

Regarding the statistical analysis, it was also performed by using the MEGGE protocol (MEGGE, 1997). Following the same approach explained in previous Section 5.3.1, MG and VG values were calculated and values are listed in Table 5.8.

Table 5.8: Statistical performance and evaluation for groups with 1.5 m/s of wind speed (Figure 5.17) at values of leak rate specified

Case	MG	VG	FAC2
N	1.03	1.01	1.04
S	1.09	1.08	1.13
E	1.28	1.16	1.35
W	1.21	1.09	1.25
NE	1.16	1.04	1.17
SE	1.17	1.04	1.18
SW	1.31	1.11	1.33
NW	1.01	1.00	1.01

Figure 5.18 shows the values of MG and VG compiled in the same graph. Hence, the use of the MEGGE approach to evaluate the performance of the M-02 model also provided good results and a good agreement with the numerical data.

Although the values of MG and VG were closer to unity in the first proposed model, the second model represented a better description of the dispersion phenomena.

The new M-02 model is recommended for calculation of flammable volumes due to

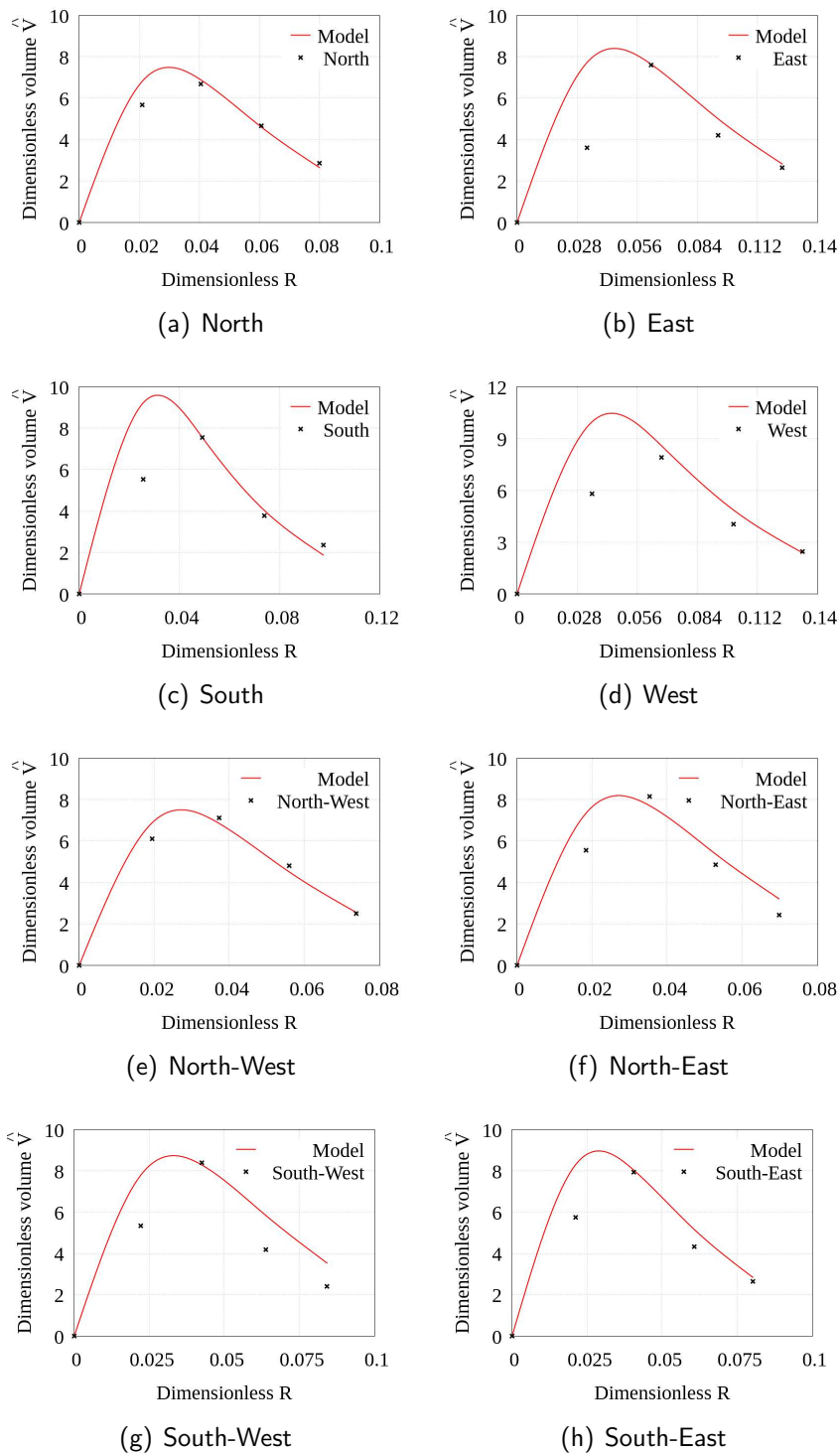


Figure 5.17: Comparison between $\hat{V}(R)$ model and \hat{V} at different values of leak rate of 25, 48, 72, and 95 kg/s at 1.5 m/s of wind speed considering the eight wind directions and at up leak direction.

its accuracy, accessibility and ease to handle. This model is very convenient when it comes to industrial applications because only considers the adjustment of two variables, and the simulation of a few dispersion scenarios to have a flammable cloud trend.

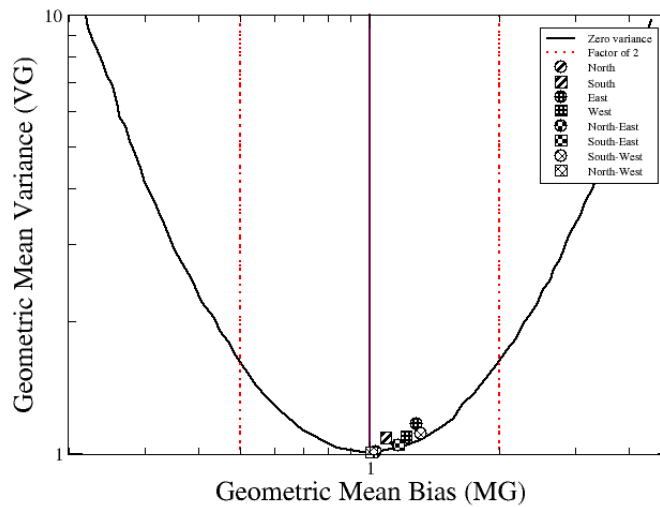


Figure 5.18: Geometric mean bias against geometric mean variance

In this regard, by employing computational tools such as the Monte Carlo approach, the calculation of flammable cloud volumes of countless scenarios will become effortless and easy to predict. The Appendix C presents an engineering procedure to the application of the new model M-02 for calculation of flammable cloud size.

5.4 The Monte Carlo Method Applied in Dispersion Analysis

The idea behind the use of the Monte Carlo method for dispersion analysis, lies in calculating countless values of V_f and simulates several dispersion scenarios at the same time.

This method can be developed and executed in a MS-Excel template by following the steps below:

- **Determination of parameters for analysis:** Assuming that $V_f = (\dot{q}, \rho, \theta, \beta)$, where \dot{q} is leak rate, ρ the density, θ the leak direction, and β the wind direction.
- **Probability of occurrence:** Based on an offshore statistical database (e.g., DNV failure frequency (DNV, 2020), Metaocean (PETROBRAS, 2016), and HSE (Health and Safety Executive) (HSE, 2001) establishes for each value of leak rate, wind direction and wind speed a probability of occurrence.

- **Simulation of reference:** By performing some ventilation simulations in FLACS, we obtained the VA (ventilation rate) value. In this sense, we will have the VA and the wind speed of reference for further VA calculations to new wind speed values with Equation 5.3.
- **Monte Carlo method in MS-Excel:** We started by setting a random number. This random number is compared with probability values. For example, we have to attribute a probability value for each leak rate set. The determination of the absolute value of the lowest random number closer to a certain probability will correspond to the right leak rate. The same reasoning can be used for calculations of wind speed and wind direction.
- **Calculation of ventilation rate (VA):** For each value of wind speed (U), we need to calculate its corresponding VA with the following equation:

$$\frac{VA_{ref}}{U_{ref}} U_{new} = VA_{new} \quad (5.3)$$

- **Calculation of R:** At the conditions of leak and wind established in the analysis, we need to adjust A and B for $\hat{V}(R)$ calculations.

$$\hat{V}(R) = [A^2 \exp(-RB)] R^{\frac{3}{2}} \quad (5.4)$$

$$\hat{V} = \frac{u^{3/2} \rho^{3/2} V_f}{\dot{q}^{3/2}} \quad (5.5)$$

$$R = \frac{\dot{q}}{\rho VA} \quad (5.6)$$

With values of A and B and using the Equation 5.6, values of \hat{V} are calculated for each scenario simulated. Then, replacing with Equation 5.4, values of R are obtained.

- **Calculation of flammable cloud volume (V_f):** By using the Equation 5.5, we calculated V_f . With this methodology, for a given leak rate, we will have a corresponding wind direction, wind speed, VA, R, A and B, $\hat{V}(R)$, and V_f . In this sense, there will not be needed to perform a higher amount of simulations, and the computational cost will decrease considerably.

After following this procedure, values of V_f are obtained with a very good degree of accuracy respect to the CFD data. An example of the application of the Monte Carlo Method for flammable cloud volume calculations is shown in Appendix B.

Chapter6

Conclusion and Future Work

6.1 Main Findings

The current dissertation presented two physical models based on dimensional analysis. Firstly, an analysis of various parameters concerning the dispersion of the flammable cloud suggested an oscillating behavior. Given the number of independent parameters, the first proposed model comprises two terms. The first term is due to the sinusoidal pattern of the CFD findings, while the second part represents an exponential growth of the cloud for certain number of parameters.

The second model indicates an exponential trend that decays over time. This behavior may be explained based on the dynamics of the flammable cloud volume. That is, when the amount of gas inside the module is high, a flammable cloud size is rapidly formed. As long as the cloud attains its highest point (in terms of flammability limits), after a period, the flammable gas cloud decays because it exceeds the upper flammable limit (UFL), becoming too rich to burn.

The new M-02 model showed to have a very good agreement for R ranging from 0.1 to 0.04 leading to top clouds. The investigation has also demonstrated that the predicted values by the M-02 model had better agreement with the CFD results than the M-01 model.

The scatter presented in the study of the accuracy of the first model emphasizes the influence of the relevant parameters, previously discussed through this dissertation, in the evaluation of flammable cloud volumes.

The models developed show to be a promising alternative in the calculation of the flammable cloud volume. By the implementation of the M-02 model, industries can have several advantages. These advantages include less computational effort, best representation of the dispersion phenomena, and calculation of countless values of flammable cloud volume in short time with high level of accuracy.

The purpose of this work lied in developing a novel alternative on the underlying physics that governs the dispersion phenomena to predict flammable cloud volumes. Dr. Vianna's lab (L4R1S4) at UNICAMP, developed a computational tool named McPEAS under

the Petrobras project. This tool uses the M-02 model for flammable volume calculations with a high level of accuracy. The contribution made by this dissertation led to perform a wide range of scenario's simulations and predict volumes in short periods. Overall, the M-02 model helped in minimizing the computational time in executing dispersion analysis for probabilistic explosion studies.

Ultimately, it was observed that the hypothesis was reached successfully, because it was possible to obtain two mathematical and physical correlations to describe and study the dispersion phenomena, both model agreements were extremely good.

6.1.1 Recommendations in Future Work

As future work, researchers may consider evaluating the incidence of turbulence intensity with the cloud size. Furthermore, some future ideas recommended to tackle are:

1. Investigate about other applications of the dimensionless number and determine its restrictions in the analysis of the cloud behavior
2. Improve the M-02 model by adding parameters that count the turbulent influence as the wind speed varies

6.1.2 Scientific Production

1. One published article in the Journal of Loss Prevention for Process Industries (*Leak release momentum and the convective flow influence on the calculation of flammable cloud*)
2. Two congress presentations, in which one of them presented at the international symposium at the Mary Kay O'Connor Process Safety Center (MKOPSC)
3. Two articles in production, one related to the alternative model development and the other presented at the MKOPSC
4. A computational tool called McPEAS for the Petrobras project offering accurate calculation of V_f

Bibliography

ANSYS. *Fluent User's Guide*. United States: ANSYS, Inc, 2011.

AZZI, C.; ROGSTADKJERNET, L.; WINGERDEN, K.; CHOI, J.; RYU, Y. Influence of scenario choices when performing cfd simulations for explosion risk analyses: Focus on dispersion. *Journal of loss prevention in the process industries*, v. 41, p. 87–96, 2016.

BURTON, R. *Atmospheric dispersion modelling. Course given in master in Computational Fluid Dynamics*. 1998.

CROWL, D.; LOUVAR, J. *Chemical Process Safety: Fundamentals with Applications*. Third edition. United States: Prentice Hall PTR, 2011.

DASGOTRA, A.; TEJA, G.; SHARMA, A.; MISHRA, K. Cfd modeling of large-scale flammable cloud dispersion using flacs. *Journal of Loss Prevention in the Process Industries*, v. 56, p. 531–536, 2018.

DEVAULL, G.; KING, J.; LANTZY, R.; FONTAINE, D. *Understanding atmospheric dispersion of accidental releases. A CCPS concept book*. American Institute of Chemical Engineers: Wiley-AIChE, 1995.

DNV, D. N. V. *Failure frequency guidance: process equipment leak frequency data for use in QRA*. London: DNV, 2020.

ECKHOFF, R. *Explosion Hazards in the Process Industries (Second Edition)*. Second edition. UK & USA: Gulf Professional Publishing, 2016.

FERREIRA, T.; SANTOS, R.; VIANNA, S. A coupled finite volume method and gilbert johnson keerthi distance algorithm for computational fluid dynamics modeling. *Comp. Methods Appl. Mech. Eng.*, v. 352, p. 417 – 136, 2019.

FERREIRA, T.; VIANNA, S. A novel coupled response surface for flammable gas cloud volume prediction. *Int. J. Model. Simul. Petrol. Ind.*, v. 8, p. 8 – 16, 2014.

FIATES, J.; VIANNA, S. Numerical modeling of gas dispersion using openfoam. *Process Safety Environmental Protection*, v. 104, p. 277 – 293, 2016.

FOX, R.; PRITCHARD, P.; MCDONALD, A. *Introduction to Fluid Mechanics, 7th Ed*. USA: Wiley India Pvt. Limited, 2009.

GEXCON. *FLACS v10.8 User's Manual*. Norway: Gexcon AS, 2018.

GUPTA, S.; CHAN, S. Cfd based explosion risk analysis methodology using time varying release rates in dispersion simulations. *Journal of loss prevention in the process industries*, v. 39, p. 59–67, 2016.

HISKEN, H.; LAKSHMIPATHY, S.; ATANGA, G.; SKJOLD, T. *Technical note: model evaluation protocol for HySEA*. [S.l.]: Gexcon AS, 2016.

HSE. *Offshore hydrocarbon release statistics. HID statistics report HSR 2001002*. [S.l.]: HSE, 2001.

- JIN, Y.; JANG, B. Probabilistic explosion risk analysis for offshore topside process area. part i: a new type of gas cloud frequency distribution for time-varying leak rates. *Journal of Loss Prevention in the Process Industries*, v. 51, p. 125–136, 2018.
- KANG, K.-Y.; CHOI, K.-H.; CHOI, J. W.; RYU, Y. H.; LEE, J.-M. Dynamic response of structural models according to characteristics of a gas explosion on the topside platform. *Ocean Engineering*, v. 113, p. 174–190, 2016.
- KUNDU, P.; COHEN, I. *Fluid Mechanics*. San Diego, USA: Academic Press, 2002.
- MALISKA, C. *Transferência de Calor e Mecânica dos Fluidos Computacional*. Rio de Janeiro, BR: Livros Técnicos e Científicos Editora S.A, 2004.
- MEGGE. *CEG: gas explosion model evaluation protocol*. [S.l.]: European Communities, 1997.
- PATANKAR, S. *Numerical Heat Transfer and Fluid Flows*. United States of America: Series in Computational Methods in Mechanics and Thermal Sciences, 1980. 197 p.
- PETROBRAS. *Technical specification (2005). Metocean data. I-ET-3000.00 -1000-941-PPC-001*. [S.l.]: Petrobras, 2016.
- QIAO, A.; ZHANG, S. Advanced cfd modeling on vapor dispersion and vapor cloud explosion. *Journal of loss prevention in the process industries*, v. 23, p. 843–848, 2010.
- SCOTT, D.; HANSEN, O.; GAVELLI, F.; BRATTETEIG, A. *Using CFD to analyze gas detector placement in process facilities*. 2011.
- SHI, J.; LI, J.; KHAN, F.; ZHU, Y.; LI, J.; CHEN, G. Robust data-driven model to study dispersion of vapor cloud in offshore facility. *Ocean Engineering*, v. 161, p. 98–110, 2018.
- SHI, J.; LI, J.; ZHU, Y.; HAO, H.; CHEN, G.; XIE, B. A simplified statistic-based procedure for gas dispersion prediction of fixed offshore platform. *Process Safety and Environmental Protection*, v. 114, p. 48–63, 2018.
- SPICER, T. O.; HAVENS, J. Application of dispersion models to flammable cloud analyses. *Journal of Hazardous Materials*, v. 49, n. 2, p. 115 – 124, 1996.
- VERSTEEG, H.; MALALASEKERA, W. *An introduction to computational fluid dynamics: the finite volume method*. England: Pearson Education, 2007.

Appendix A Additional Numerical Data

A.1 Visualization of CFD results

The following figures represent the worst-case scenarios of the first set of simulations. The velocity vector in m/s (VVEC) and the fuel mass fraction which are parameters given by FLACS are visualized here. The flammability limit was considered for methane from 0.05 (5%) to 0.15 (15%) to set the visualization,

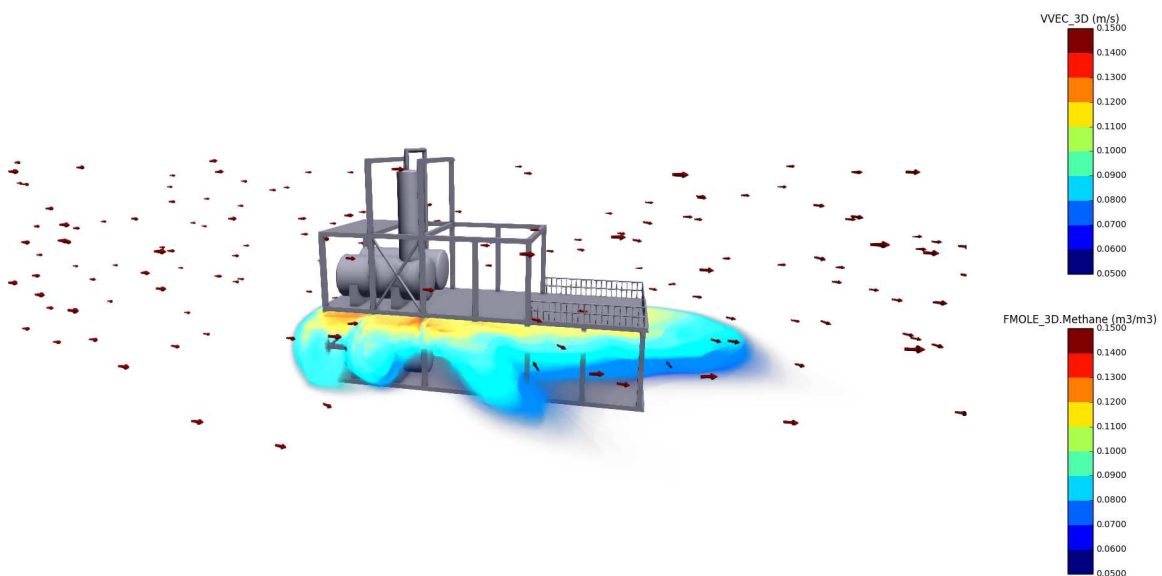


Figure A.1: First set of dispersion scenarios at 70 seconds after the release: variations of wind direction at up leak jet direction with a $2080 m^3$ of flammable cloud volume

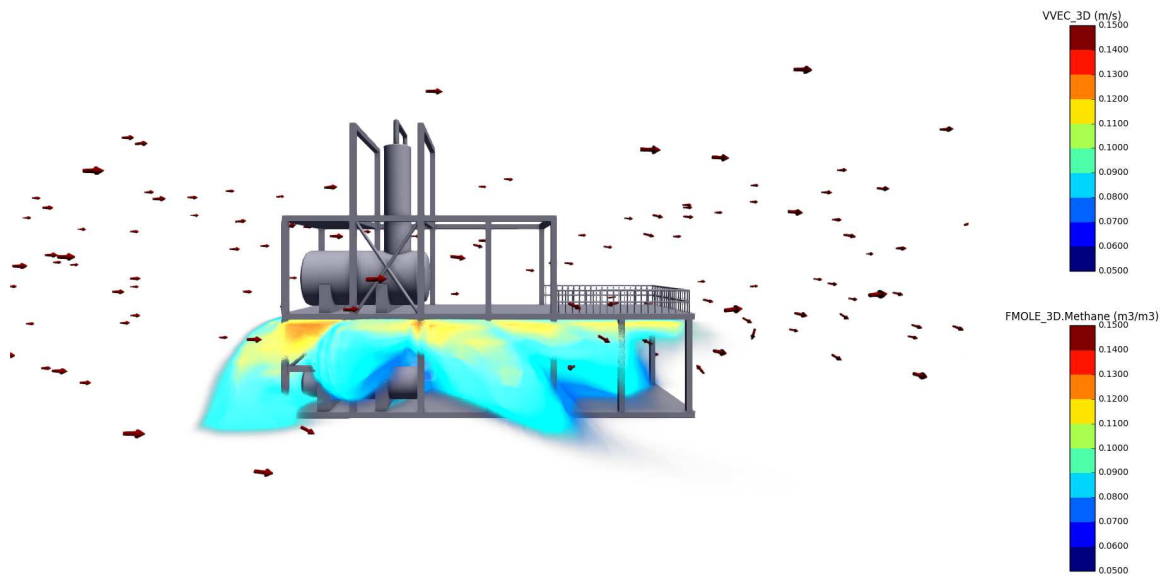


Figure A.2: First set of dispersion scenarios at 70 seconds after the release: variations of wind speed at up leak jet direction with a 2460 m^3 of flammable cloud volume

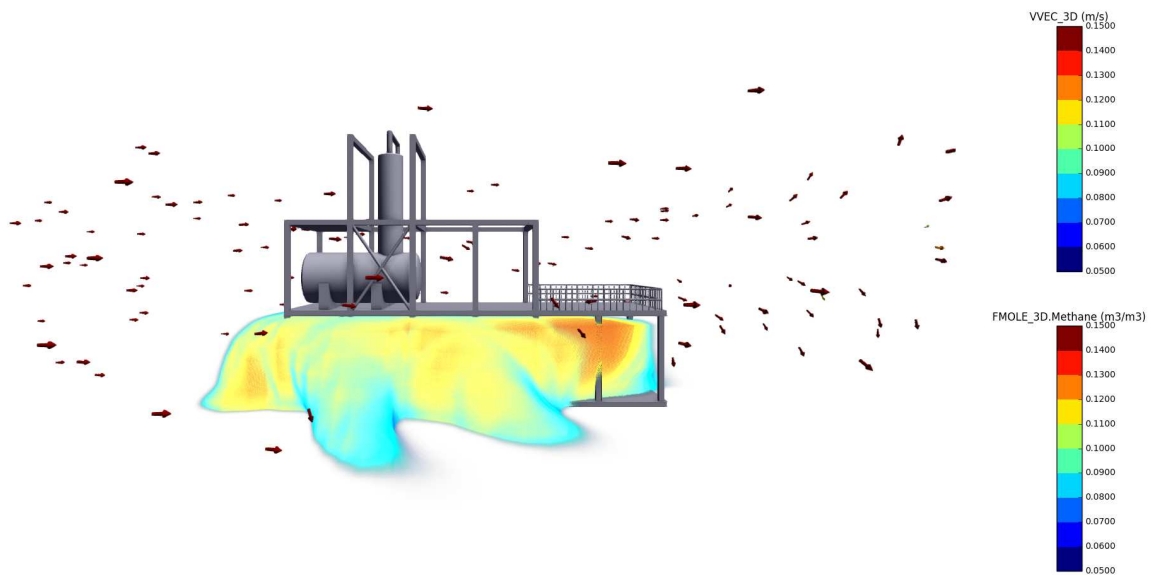


Figure A.3: First set of dispersion scenarios at 70 seconds after the release: variations of leak rate at up leak jet direction with a 1800 m^3 of flammable cloud volume

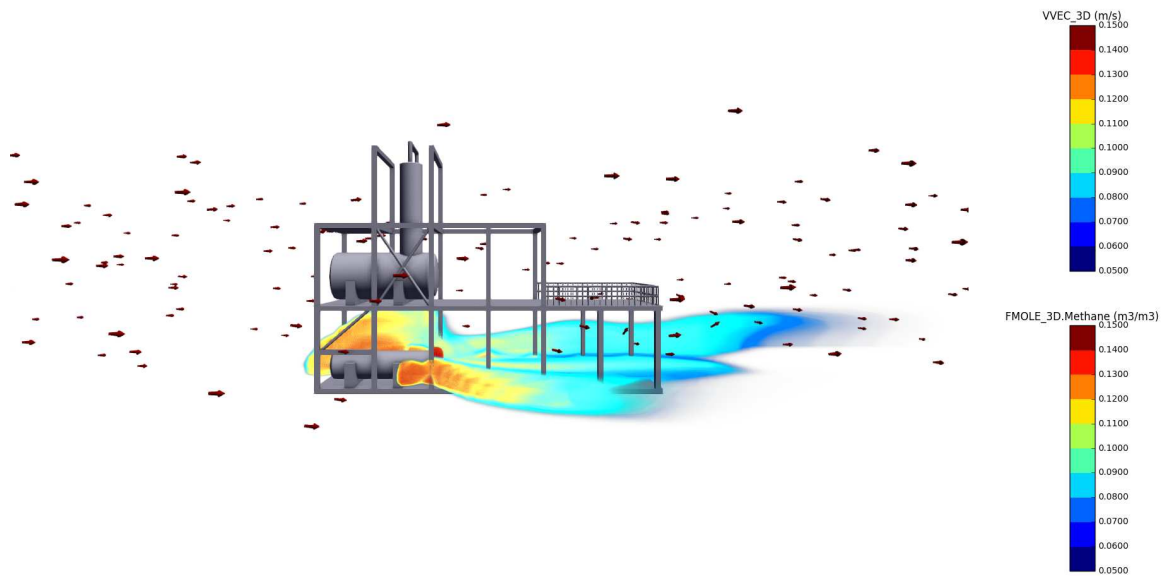


Figure A.4: First set of dispersion scenarios at 70 seconds after the release: variations of leak rate at down leak jet direction with a 520 m^3 of flammable cloud volume

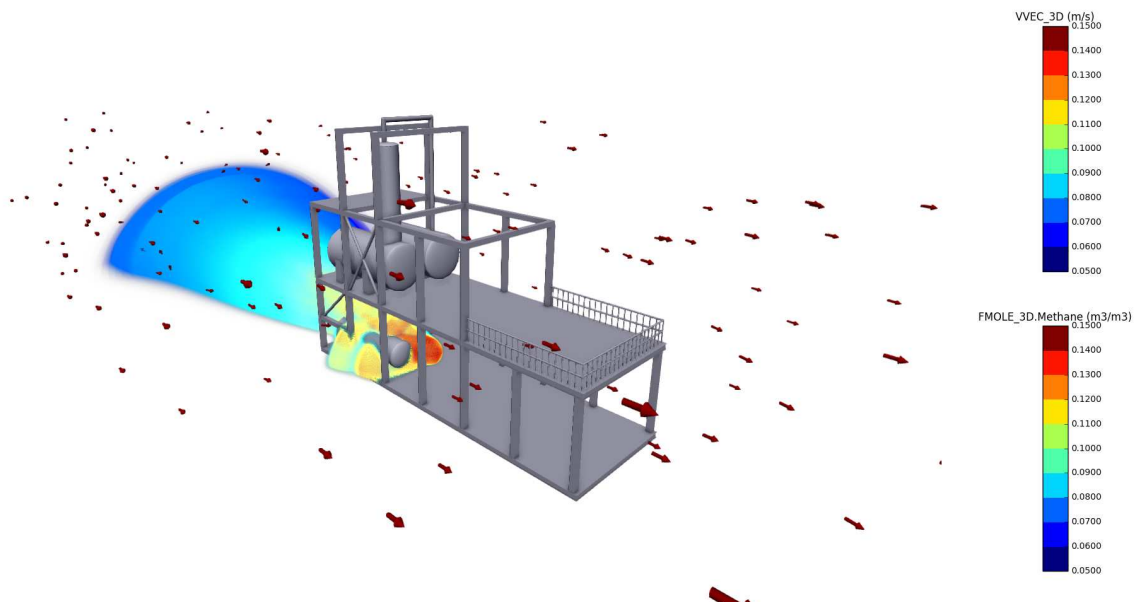


Figure A.5: First set of dispersion scenarios at 70 seconds after the release: front leak directions with a 443 m^3 of flammable cloud volume

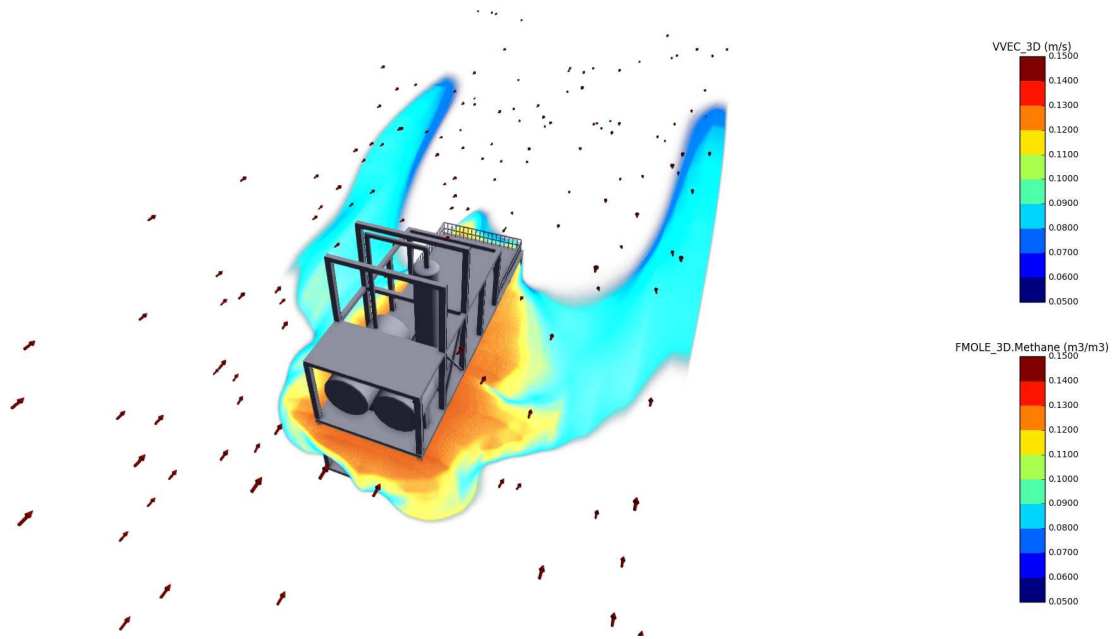


Figure A.6: First set of dispersion scenarios at 70 seconds after the release: up leak directions with a 1780 m^3 of flammable cloud volume

A.2 Dimensional results

Table A.1: Value of Q_9 and \hat{V} for the first set of dispersion scenarios

Groups	Input				Output	
	Leak rate (kg/s)	Wind speed (m/s)	Leak direction	Wind direction	Maximum Q_9 (m ³)	\hat{V}
Group 1A	50	6	Up	N	804,0	23,9
	50	6	Up	S	862,0	25,64
	50	6	Up	E	894,0	26,59
	50	6	Up	W	2080,0	61,87
	50	6	Up	NE	1040,0	30,93
	50	6	Up	SE	691,0	20,55
	50	6	Up	SW	1620,0	48,19
	50	6	Up	NW	1590,0	47,29
Group 1B	50	1	Up	W	1150,0	2,33
	50	2	Up	W	1630,0	9,33
	50	4	Up	W	2460,0	39,83
	50	8	Up	W	1140,0	52,21
	50	10	Up	W	636,0	40,70
	50	12	Up	W	499,0	41,98
Group 2A	0.5	3	Up	W	0,9	9,51
	1	3	Up	W	2,8	10,37
	5	3	Up	W	47,7	15,86
	10	3	Up	W	212,0	24,93
	15	3	Up	W	525,0	33,60
	25	3	Up	W	1060,0	31,53
	100	3	Up	W	1800,0	6,69
	150	3	Up	W	1350,0	2,73
	200	3	Up	W	1660,0	2,18
	250	3	Up	W	953,0	0,90
	300	3	Up	W	873,0	0,62
	350	3	Up	W	652,0	0,37
	400	3	Up	W	780,0	0,36
	450	3	Up	W	487,0	0,19
500	3	Up	W	480,0	0,16	
550	3	Up	W	591,0	0,17	
Group 2B	0.5	6	Up	W	0,5	15,68
	1	6	Up	W	1,9	19,56
	5	6	Up	W	47,7	44,87
	10	6	Up	W	96,6	32,12
	15	6	Up	W	322,0	58,29
	25	6	Up	W	609,0	51,23
	100	6	Up	W	1780,0	18,72
	150	6	Up	W	1340,0	7,67
	200	6	Up	W	1670,0	6,21
	250	6	Up	W	966,0	2,57
	300	6	Up	W	849,0	1,72
	350	6	Up	W	305,0	0,49
	400	6	Up	W	302,0	0,40
	450	6	Up	W	370,0	0,41
500	6	Up	W	328,0	0,31	
550	6	Up	W	343,0	0,28	
Group 3A	50	6	Left	W	40,7	1,21
	50	6	Right	W	43,8	1,30
	50	6	Down	W	520,0	15,47
	50	6	Front	W	416,0	12,37
	50	6	Back	W	242,0	7,20
Group 3B	100	6	Left	W	39,8	0,42
	100	6	Right	W	46,5	0,49
	100	6	Down	W	404,0	4,25
	100	6	Front	W	443,0	4,66
	100	6	Back	W	256,0	2,69

Table A.2: Value of Q_9 and \hat{V} for the second set of dispersion scenarios (part a)

Groups	Input				Output	
	Leak rate (kg/s)	Wind speed (m/s)	Leak direction	Wind direction	Maximum Q_9 (m ³)	\hat{V}
Group 4A	5	2	Up	N	27,9	5,05
	5	2	Up	S	27,8	5,03
	5	2	Up	E	31,3	5,66
	5	2	Up	W	32,3	5,85
	5	2	Up	NE	32,9	5,96
	5	2	Up	SE	28,9	5,23
	5	2	Up	SW	29,7	5,38
	5	2	Up	NW	28,0	5,07
Group 4B	5	6	Up	N	21,0	19,75
	5	6	Up	S	18,3	17,21
	5	6	Up	E	27,8	26,15
	5	6	Up	W	27,8	26,15
	5	6	Up	NE	17,5	16,46
	5	6	Up	SE	19,3	18,15
	5	6	Up	SW	19,0	17,87
	5	6	Up	NW	17,5	16,46
Group 4C	5	8	Up	N	16,6	24,04
	5	8	Up	S	13,5	19,55
	5	8	Up	E	27,8	40,26
	5	8	Up	W	27,8	40,26
	5	8	Up	NE	14,7	21,29
	5	8	Up	SE	13,9	20,13
	5	8	Up	SW	15,7	22,74
	5	8	Up	NW	14,6	21,14
Group 5A	25	2	Up	N	391,0	6,33
	25	2	Up	S	361,0	5,84
	25	2	Up	E	333,0	5,39
	25	2	Up	W	517,0	8,37
	25	2	Up	NE	473,0	7,66
	25	2	Up	SE	514,0	8,32
	25	2	Up	SW	495,0	8,01
	25	2	Up	NW	631,0	10,22
Group 5B	25	6	Up	N	268,0	22,55
	25	6	Up	S	336,0	28,27
	25	6	Up	E	163,0	13,71
	25	6	Up	W	366,0	30,79
	25	6	Up	NE	201,0	16,91
	25	6	Up	SE	275,0	23,13
	25	6	Up	SW	282,0	23,72
	25	6	Up	NW	210,0	17,67
Group 5C	25	8	Up	N	357,0	46,24
	25	8	Up	S	242,0	31,34
	25	8	Up	E	171,0	22,15
	25	8	Up	W	289,0	37,43
	25	8	Up	NE	183,0	23,70
	25	8	Up	SE	221,0	28,63
	25	8	Up	SW	266,0	34,45
	25	8	Up	NW	197,0	25,52

Table A.3: Value of Q9 and \hat{V} for the second set of dispersion scenarios (part b)

Groups	Input				Output	
	Leak rate (kg/s)	Wind speed (m/s)	Leak direction	Wind direction	Maximum Q9 (m3)	\hat{V}
Group 6A	200	2	Up	N	738,0	0,53
	200	2	Up	S	825,0	0,59
	200	2	Up	E	789,0	0,56
	200	2	Up	W	789,0	0,56
	200	2	Up	NE	764,0	0,55
	200	2	Up	SE	789,0	0,56
	200	2	Up	SW	787,0	0,56
	200	2	Up	NW	765,0	0,55
Group 6B	200	6	Up	N	739,0	2,75
	200	6	Up	S	684,0	2,54
	200	6	Up	E	795,0	2,96
	200	6	Up	W	793,0	2,95
	200	6	Up	NE	890,0	3,31
	200	6	Up	SE	828,0	3,08
	200	6	Up	SW	767,0	2,85
	200	6	Up	NW	782,0	2,91
Group 6C	200	8	Up	N	517,0	2,96
	200	8	Up	S	521,0	2,98
	200	8	Up	E	808,0	4,62
	200	8	Up	W	781,0	4,47
	200	8	Up	NE	532,0	3,04
	200	8	Up	SE	713,0	4,08
	200	8	Up	SW	681,0	3,90
	200	8	Up	NW	782,0	4,48

Table A.4: Value of Q9 and \hat{V} for the third set of dispersion scenarios

Groups	Input				Output	
	Leak rate (kg/s)	Wind speed (m/s)	Leak direction	Wind direction	Maximum Q9 (m3)	\hat{V}
Group 7A	50	2	Up	N	1510,0	8,64
	50	2	Up	S	1820,0	10,42
	50	2	Up	E	1570,0	8,99
	50	2	Up	W	1630,0	9,33
	50	2	Up	NE	1300,0	7,44
	50	2	Up	SE	1640,0	9,39
	50	2	Up	SW	1440,0	8,24
	50	2	Up	NW	1450,0	8,30
Group 7B	50	6	Up	N	804,0	23,91
	50	6	Up	S	862,0	25,64
	50	6	Up	E	894,0	26,59
	50	6	Up	W	2080,0	61,87
	50	6	Up	NE	1040,0	30,93
	50	6	Up	SE	691,0	20,55
	50	6	Up	SW	1620,0	48,19
	50	6	Up	NW	1590,0	47,29
Group 7C	50	8	Up	N	731,0	33,48
	50	8	Up	S	1360,0	62,28
	50	8	Up	E	593,0	27,16
	50	8	Up	W	1140,0	52,20
	50	8	Up	NE	945,0	43,28
	50	8	Up	SE	815,0	37,32
	50	8	Up	SW	1250,0	57,24
	50	8	Up	NW	1110,0	50,83
Group 8A	100	2	Up	N	2090,0	4,23
	100	2	Up	S	1920,0	3,88
	100	2	Up	E	1800,0	3,64
	100	2	Up	W	1800,0	3,64
	100	2	Up	NE	1720,0	3,48
	100	2	Up	SE	1690,0	3,42
	100	2	Up	SW	1690,0	3,42
	100	2	Up	NW	1880,0	3,80
Group 8B	100	6	Up	N	2290,0	24,08
	100	6	Up	S	1920,0	20,19
	100	6	Up	E	1830,0	19,24
	100	6	Up	W	1780,0	18,72
	100	6	Up	NE	912,0	9,59
	100	6	Up	SE	1110,0	11,67
	100	6	Up	SW	1470,0	15,46
	100	6	Up	NW	1470,0	15,46
Group 8C	100	8	Up	N	1790,0	28,98
	100	8	Up	S	1370,0	22,18
	100	8	Up	E	1690,0	27,36
	100	8	Up	W	1660,0	26,88
	100	8	Up	NE	930,0	15,06
	100	8	Up	SE	1020,0	16,51
	100	8	Up	SW	1350,0	21,86
	100	8	Up	NW	1380,0	22,34

Appendix B

Developed Tools for V_f Calculations

B.1 Introduction

In this section, two examples of modeling implementation are presented. Initially, it is shown a procedure to execute a case study using McPEAS (Monte Carlo Probabilistic Explosion Analysis Simulator) to perform a probabilistic explosion analysis. Finally, the Monte Carlo Method is applied in MS- Excel. The objective is to show the proposed model application and how it is employed in safety procedures.

B.2 How to Perform a Case Study with McPEAS?

B.2.1 Modeling in CFD

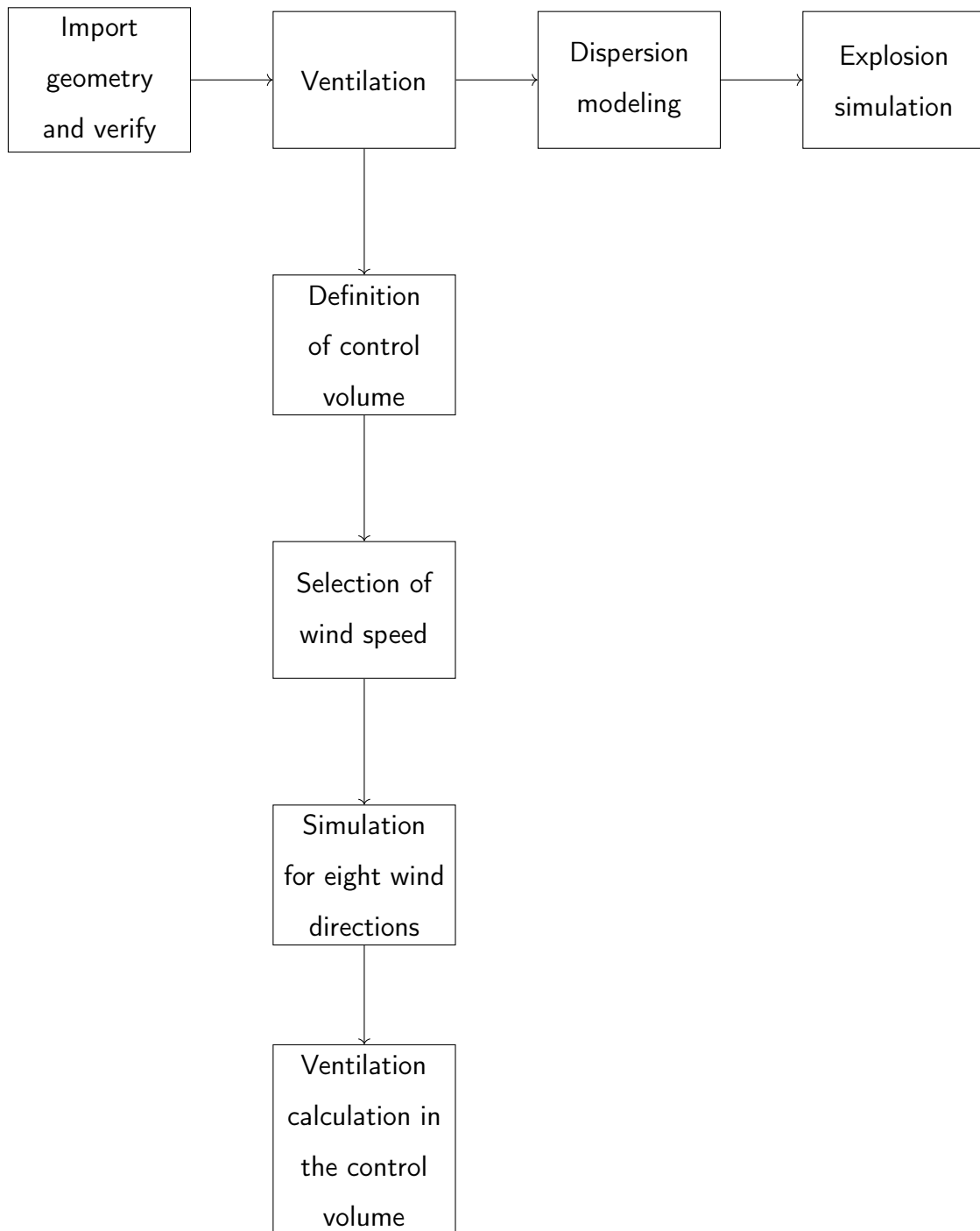
- Step 1. Simulations of ventilation, gas dispersion and explosion
- Step 2. Curve fitting for dispersion and explosion models

B.2.2 Modeling in McPEAS

- Step 3. Adjustment of input parameters in McPEAS (refer to Figure B.1)
- Step 4. Elaboration of exceedance curves from Monte Carlo simulations

B.3 McPEAS Procedure Execution

Step 1. Geometry



Step 2. Dispersion

- Definition of gas composition
- Leak temperature calculation
- Gas compressibility calculation
- Dispersion simulation for a representative segment
- R calculation (dimensionless leak rate)
- Flammable cloud volume calculation

Step 3. Explosion

- Simulation of explosion scenarios until 5% filling degree of the control volume from the largest cloud (regular intervals)
- The cloud location must reflect the dispersion study
- Two ignition points must be considered (in the middle and at the edge of the cloud)

Step 4. Curve's fitting

- Based on CFD data, tune the model $\hat{V}(R)$
- Perform a verification of at least three additional cases

Step 5. McPEAS application

- Gas properties, control volume, leak rate frequency, In built-gas (step 1: Figure B.1)
- Automatic input of meteorological data, data adjustment (step 2: Figure B.2)
- Application of dispersion and explosion models (step 3: Figure B.3)
- Monte Carlo simulation, selection of leak rate, selection of wind conditions, cloud volume calculations, exceedance curve (step 4: Figure B.4)

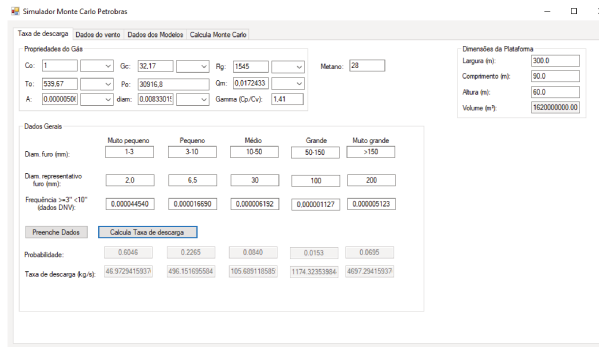


Figure B.1: Step 1 in McPEAS Software

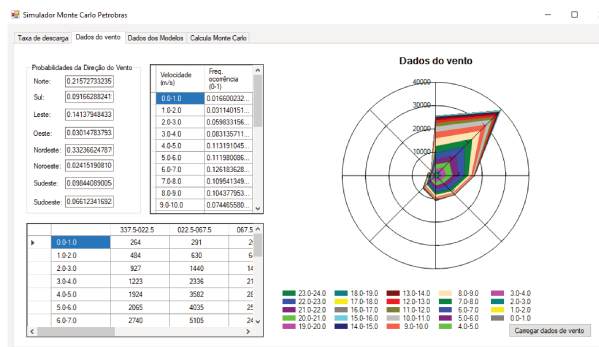


Figure B.2: Step 2 in McPEAS Software

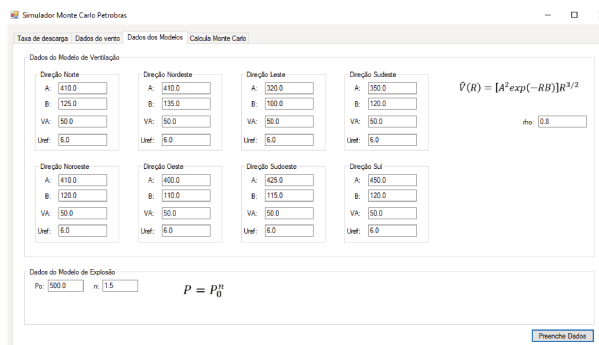


Figure B.3: Step 3 in McPEAS Software

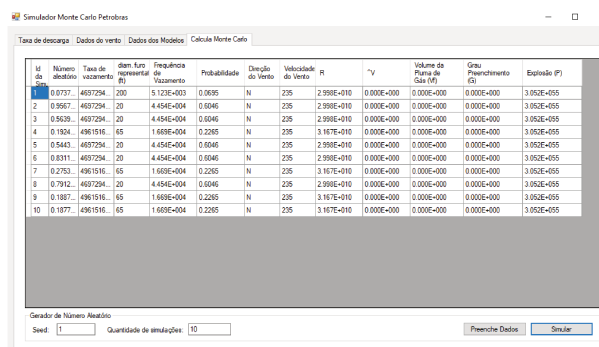


Figure B.4: Step 4 in McPEAS Software

Appendix C

How to Use the M-01 and M-02 Proposed Models?

C.1 The M-01 Proposed model

The M-01 proposed model, can be used as follows:

1. Perform CFD simulations and use the variables (A, B, amplitude, and mean) developed (refers to Table C.1) for all leak directions. The user also can adjust the four variables at its process conditions. In this latter, some simulations are needed to determine them and finally tune the model

Table C.1: Developed variables for the proposed model at all leak directions

Developed variables	Leak Directions					
	Up	Back	Left	Right	Down	Front
A	180.03	178.13	180.35	180.36	180.73	179.41
B	1.45	4.10	8.02	19.98	3.44	9.71
Mean	23.06	8.44	1.31	1.41	11.95	5.05
Amplitude	0.85	1.52	1.02	0.44	-0.54	3.05

2. Identify the wake conditions (volume and angle)
3. Solve the non-linear equation
4. Calculate the V_f with Equation 4.34 by replacing $\hat{V}(\beta, \alpha)$ and obtain values of flammable cloud volume

C.1.1 The M-02 Proposed Model

The M-02 proposed model, can be used by following these six steps:

1. Establish the R range based on user requirements
2. Perform CFD simulations considering the R previously set. The scenarios can be related to leak rate variations or wind speed variations. The idea is to obtain at least five points to construct the curve
3. Calculate values of \hat{V} with Equation 4.34 which is the first dimensionless number

4. Calculate the $\hat{V}(R)$ by adjusting A and B variables depend on the scenarios simulated
5. Plot the \hat{V} against $\hat{V}(R)$ to analyze the curve behavior and maximum values of \hat{V} reached
6. Calculate V_f by using the Equation 4.34 replacing the $\hat{V}(R)$ to obtain approximated values of flammable cloud volumes

The utilization of the M-02 model gives a set of curves at each wind direction, as is shown in Figure C.1. Each curve will have a maximum value of \hat{V} and a range of R where the M-02 model works in very good agreement.

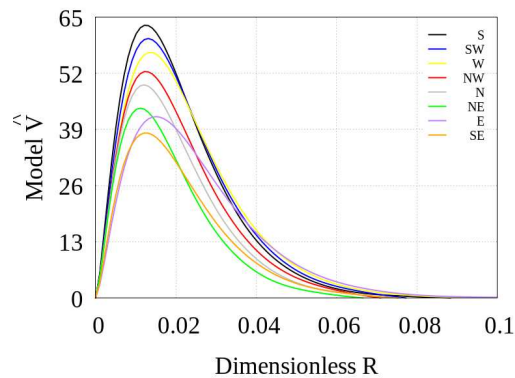


Figure C.1: Example of compilation of data of model $\hat{V}(R)$ against R for all the wind directions